The empirical probability of integrating CSP and its cost optimal configuration in a low carbon energy system of EUMENA

Author: Denis Hess[1]*

Ongoing cost reduction of low carbon energies allows an increasing implementation of such technologies for climate protection targets. How decreasing cost develop in the future is high-grade uncertain. Thus cost sensitivities analyses of an expert based cost-range are needed to show if specific technologies can be cost advantageous for an energy system. In this paper a low carbon and cost-optimal energy system of Europe, Middle East and North Africa (EUMENA) in the year 2050 is analysed with regard to concentrating solar power (CSP). Cost sensitivity analyses show how frequently an integration of CSP in the energy system is. This frequency is defined as empirical probability of technological integration (EPTI). An energy system model allows a suitable analysis framework with tangible competitive technologies such as renewable energies, nuclear power plants and carbon capture and storage (CCS). As a highlight the EPTI of an export of CSP from MENA to EU via point-to-point high voltage direct current (HVDC) transmission lines is analysed. Such CSP-HVDC power plants show an EPTI of up to 66%. CSP in MENA and southern EU show an average EPTI of 85%, nuclear power plants of 32% and CCS of 50%. The cost sensitivity analysis shows additionally the cost optimal configuration of CSP and CSP-HVDC. This clarifies the role of CSP and CSP-HVDC for the energy system as a dispatchable base and medium load power plant depending on the region inside EUMENA.

Keywords: CSP-HVDC, optimization, energy system model, renewable dispatchable energies, cost-optimal CSP configuration, DESERTEC

1   Introduction

1.1   State of science

Research activities of the DLR and other institutions depict the potential use of CSP in MENA and the transmission of CSP to Europe [1], [2], [3], [4]. They found out that the use of CSP in MENA and an export of CSP electricity from MENA to Europe via specific high voltage direct

[1] Energy Systems Analysis, German Aerospace Center (DLR), D-70569 Stuttgart, Germany.*
Corresponding author e-mail: denis.hess@dlr.de

current transmission lines (HVDC) can supplement the energy mix by balancing domestic energies such as wind turbines and photovoltaic. The progress of a worldwide CSP implementation and its potential role is shown in [5] and [6]. The authors emphasise the system value of CSP as a potential backbone of a low carbon energy system. CSP combined with thermal storage and co-firing option can provide electricity according to demand. Therefore CSP is a valuable dispatchable energy technology [7]. This distinguishes CSP from other fluctuating renewable energies in its energy quality. However, the system advantage of CSP related to cost is high-grade uncertain for a future energy system in the year 2050. Especially, with its current worldwide installed capacity of 5 GW a cost reduction is possible due to learning effects with higher installation capacities but uncertain how its cost develops in competition to other technologies. This provokes the question if a further integration of CSP can be cost advantageous on the long term perspective? Here we show with an energy system model the empirical probability of technological integration (EPTI) of CSP in a low carbon energy system in the year 2050. Energy system models are today's methods to approximate optimal future energy systems. Often they follow the target function of minimal system cost, perfect foresight and linear programming (REMix, PLEXOS, TIMES, ReEDS, etc. [8]). These numerical models are bottom-up models using detailed technology modules building up a simulation of an energy system. The minimization of system cost as objective function results in potential exclusions of specific technologies. Due to small and quite fortuitous cost difference among technologies, some technologies can be excluded automatically by the optimization model due to a small cost difference. This so-called "penny flip" effect is a major barrier in optimizing energy systems because it leads to unrealistic results. To solve this barrier as well as the uncertainty of specific technological cost, a comprehensive cost sensitivity analysis is applied.

1.2 Novelty and scientific contribution

The present paper considers a broad range of techno-economic expert assumptions. With such data a frequency of an integration of a certain technology compared to all other used technologies is possible. This empirical probability of technological integration analysis includes uncertainty and high spatio-temporal resolution applying a numerical energy system model. As a major novelty in energy system modelling and CSP analysis, this approach allows assessing the potential of an integration of a technology in a cost-optimized and low carbon energy system. Additionally, the cost-optimal configuration of CSP with its thermal storage, solar field and co-firing option is shown. Such configuration values are important for the design of this technology in an entire energy system under a least-cost assumption. As a novel highlight, CSP power plants are considered that transfer dispatchable energy from

MENA to EU via point-to-point HVDC from a CSP hotspot to a potential centre of demand in the EU.

2 Methodology and key assumptions

2.1 Hypothesis

An empirical probability of technological integration analysis can show how probable an integration of a certain technology is in a cost-optimal framework of an energy system. For this purpose an energy system model is applied with cost sensitivity scenarios of the analysed technology and tangible alternative technologies using expert cost assumptions. For CSP a learning curve approach of cost reduction is applied based on scenarios of worldwide installed capacity in the year 2050 (see appendix Table 18). Having a more detailed look on potential competitive and tangible low carbon dispatchable technologies to CSP, the EPTI of nuclear power plants and CCS technologies is calculated.

In the last part of this paper the CSP-HVDC and CSP configuration values out of the sensitivity scenarios are analysed identifying the role of the technology for the energy system in different regions.

The objective of the analysis is to model CSP relative conservatively compared to other technologies. This facilitates a conservative examination of this technology to analyse its EPTI strictly avoiding an overestimation of this technology.

2.2 Modelling framework

2.2.1 Examination area EUMENA

Calculating the EPTI for CSP the examination area EUMENA is applied. This geographical region consists of geographical sub-regions: Europe, Middle East and North Africa [9]. As a region with about 15% of global population in 2050 [10], EUMENA influences global climate targets significantly and therefore needs careful considerations on the composition of its future energy systems.
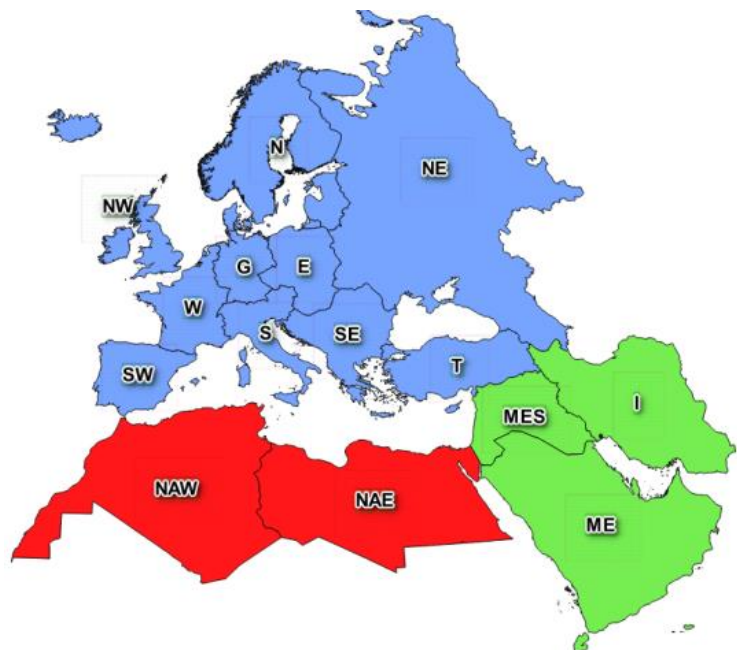

Figure 1: EUMENA geographical map

In Figure 1 the 15 analysed regions inside EUMENA are illustrated. The blue area represents geographical Europe, the green area Middle East and the red area North Africa. An aggregation inside such regions is made due to computational constraints of the used energy system model. In the following Table 1 the spatial aggregation for the model regions of the nodes in Figure 1 and the assumed annual electrical net demand is shown. The definition and abbreviation of the nodes in Table 1 is essential to better understand the results in Figure 4, Figure 5 and Figure 6. The spatial focus of the analysis is not only on the entire EUMENA region but also on sub-regions and nations, wherefore Germany is used as a national example.

An aggregation of separate nations can lead to a smoothing of their demand and resource characteristic. To reduce such falsification an aggregation is at first made according to a similar distribution of demand. Secondly the aggregation is made to limit the east-west expansion of a region avoiding an excessive smoothing of solar resources. Depending on the spatial proximity of a model region to Germany, the model regions close to Germany have a smaller spatial area than the distant model regions. This allows a better model framework to cope with a higher influence of the surrounding regions for Germany. The annual electrical net demand in 2050 follows a demand model which includes electricity demand of the heat and mobility sector and is described in the appendix in section 8.1.2 and Table 9.

Table 1: Aggregation of countries to 15 model regions in the examination area EUMENA

Model region / Node	Alias	Country or region	Annual electrical net demand [TWh] in 2050
G	Germany	Germany	706
N	North	Denmark, Norway, Sweden, Finland, Lithuania, Latvia, Estonia	571
E	East	Poland, Czech Republic, Slovakia, Hungary	429
S	South	Switzerland, Austria, Liechtenstein, Italy, Slovenia	689
W	West	France, Belgium, Netherlands, Luxemburg	920
NW	North West	United Kingdom, Ireland, Iceland	785
NE	North East	Ukraine, Moldova, Belarus, Russia until Ural mountains, Azerbaijan, Armenia, Georgia	1037
SE	South East	Greece, Croatia, Rumania, Serbia, Kosovo, Albania, Macedonia, Bulgaria, Bosnia-Herzegovina, Montenegro	321
SW	South West	Portugal, Spain	342
T	Turkey, Cyprus	Turkey, Cyprus	613
MES	Mesopotamia	Israel, Jordan, Palestine, Lebanon, Syria, Iraq	950
I	Iran	Iran	874
ME	Middle East	Djibouti, Yemen, Oman, Saudi Arabia, UAE, Qatar, Bahrain, Kuwait	974
NAE	North Africa East	Libya, Egypt	1178
NAW	North Africa West	Morocco, Algeria, Tunisia	674

2.2.2 The concept of a CSP transfer from MENA to EU

Figure 2 illustrates the concept of point-to-point transmission lines from potential CSP hotspots in MENA to centres of demand in EUMENA. The point-to-point lines from potential CSP power plants in MENA to centres of demand in EU are configured as HVDC keeping transmission losses low. A CSP-HVDC power plant is a dispatchable solar thermal power plant combined with thermal storage, co-firing option and a HVDC point-to-point transmission line. The combined and enclosed use of CSP and HVDC is defined as CSP-HVDC power plant in the following. This technology is ready for use and its elements are in operation worldwide for many years so far. The important point of view is that such a power plant includes the HVDC transmission line and is therefore projectable as a possible business case. CSP-HVDC has to be considered as a power plant in distance, just with a longer line from the generator to the feed-in point into the grid.
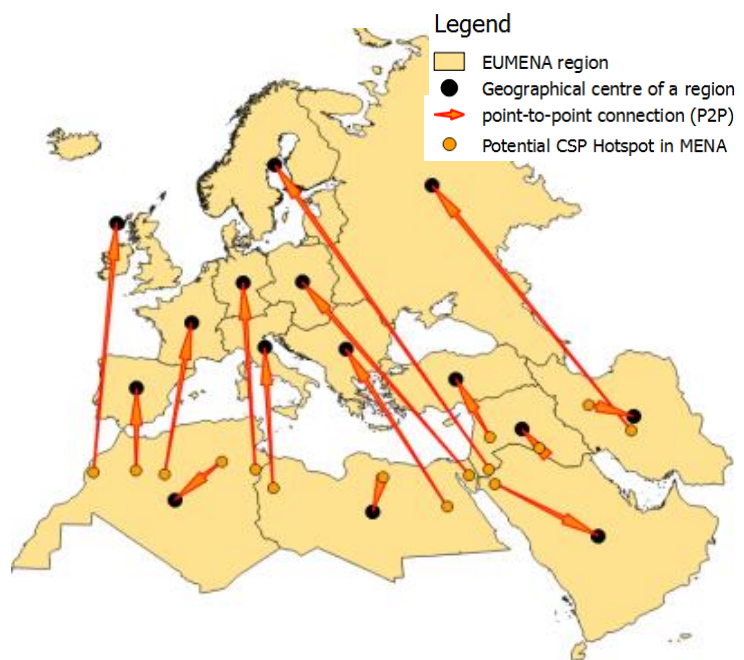
Figure 2: Scheme of CSP and point-to-point transmission lines

The total average length of such point-to-point HVDC lines to one model region is between 1200km and 3800km and is listed in Table 2. For the sensitivity analysis two pathways are used: predominant overhead lines (OHL) and predominant sea and underground cables (UGC). The pathways are calculated with a line laying model which is described in the appendix.

Table 2: CSP-HVDC transmission line lengths to model regions as potential offtakers

Model region	Predominant OHL configuration		Predominant sea and UGC configuration		Total average length of point-to-point line
	Length line land	Length line sea	Length line land	Length line sea	
G	2343	249	1212	1403	2604
N	3461	331	1675	1915	3691
E	2549	356	1104	1626	2818
S	1540	366	568	1321	1898
W	2178	214	1012	1318	2361
NW	2747	930	645	3291	3807
NE	2502	109	1342	1129	2541
SE	1928	441	587	1604	2280
NAE	0	0	0	0	0
NAW	0	0	0	0	0
SW	1206	88	521	846	1331
T	899	255	406	838	1199
MES	0	0	0	0	0
I	0	0	0	0	0
ME	0	0	0	0	0

2.2.3 Energy system model REMix

As a numerical energy system model REMix (sustainable Renewable Energy Mix) [11], [12] and [13] is applied. This bottom-up model has the target function of minimizing system cost (total cost) using linear programming under perfect foresight. System cost include the annuities of investment and the cost of operation and maintenance (O&M), fuel and emission cost for energy relevant technologies (power plants, storage and grid) shown in Eq. (1). REMix consists of two models: REMix-EnDAT (Energy Data Analysis Tool) and REMix-OptiMo (Energy System Optimization). REMix-EnDAT uses climate and weather data to calculate potentials and technological time series of PV, Wind, CSP and hydro power plants. By regarding the cost of technologies, REMix-OptiMo can decide upon configuration and operation of the energy system. This means a quantitative decision about which capacity is built and which dispatch is used. Such an optimization can be performed based on a "greenfield" (model endogenous optimization), a "partial greenfield" (model endogenous

optimization under exogenously given capacities) or just a dispatch optimization with only exogenously given capacities. REMix-OptiMo performs the following output data: capacity, generation, system operation, cost as well as emission data. The model structure is illustrated in Figure 3. REMix is built in the algebraic language GAMS using the CPLEX solver. A detailed overview of the model methods is available in the references [11], [12] and [13]. Due to worldwide available meteorological data, calculated and complied by the German Aerospace Centre, REMix is worldwide applicable. The basic modelling assumptions including the CSP model and all applied and tangible technologies such as renewable energies, nuclear power plants, CCS, coal power plants and gas turbines are explained and characterised in the appendix.
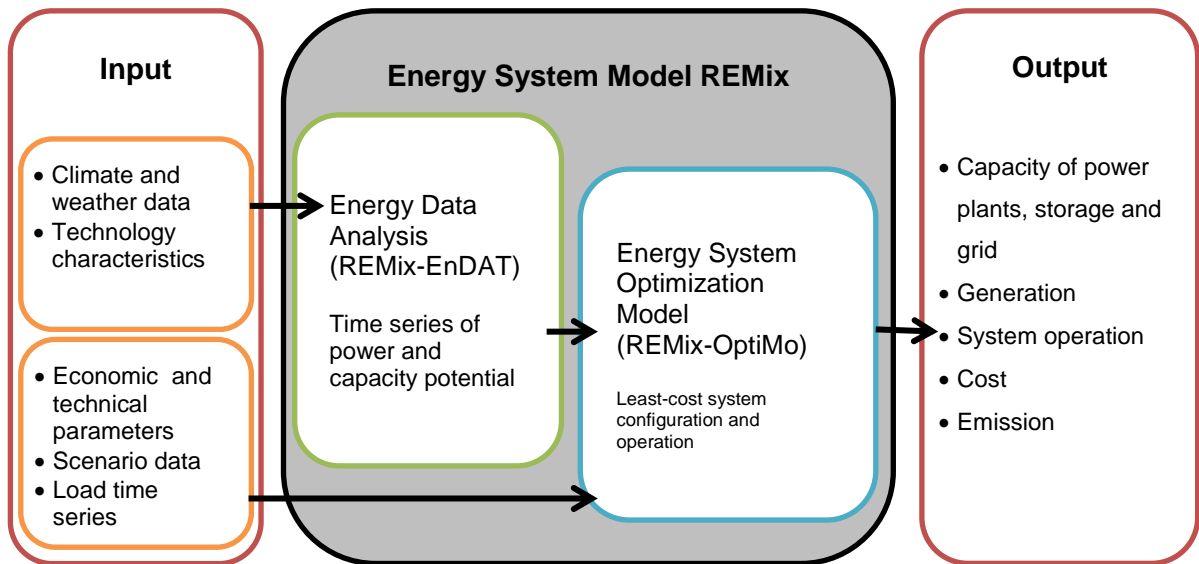

Figure 3: Model structure of REMix-EnDAT and REMix-OptiMo, input and output data based on [13]

Objective function in the linear program framework to be minimized:

$$\sum System\ cost\ [k€]\ \rightarrow minimize \tag{1}$$

The following equations concretise the system cost and calculation method. REMix, can optimize the variables which are written in bold. System cost is the sum of capital cost $C_{capital}$ and operation cost $C_{operation}$ described in Eq.(2). For the calculation of capital cost the annuity method is used including endogenous capacity $P_{addedCap}$ and exogenous capacity $P_{existCap}$ according to Eq. (3) and (4), which are multiplied with specific cost $c_{specInv}\ \left[\frac{\%\ of\ investment}{year}\right]$. The operation cost of the power plant park is calculated using fix

and variable O&M as well as fuels and emission cost according to Eq. (5). All cost assumptions in the paper are given in constant monetary value of the year 2015.

$$System\ Cost\ [k€] = \boldsymbol{C}_{capital} + \boldsymbol{C}_{operation} \tag{2}$$

$$= Capital\ Cost + Fix\ O\&M\ Cost + Variable\ O\&M\ Cost + Fuel\ Cost + Emission\ Cost$$

$$\boldsymbol{C}_{capital} = \left(\boldsymbol{P}_{addedCap} + P_{existCap}\right) \cdot c_{specInv} \cdot f_{annuity} \tag{3}$$

$$f_{annuity} = \frac{i \cdot (1+i)^{t_y}}{(1+i)^{t_y} - 1} \tag{4}$$

$$\boldsymbol{C}_{operation} = \left(\boldsymbol{P}_{addedCap} + P_{existCap}\right) \cdot c_{specInv} \cdot c_{O\&M\ Fix} \tag{5}$$

$$+ \sum_t \boldsymbol{P}_{gen}(t) \cdot (c_{O\&M\ Variable} + c_{Fuel} + c_{Emission})$$

The used parameters for Eq. (2)-(5) are available in the appendix in Table 12 to Table 16.

2.3 Empirical probability analysis within an energy system model

The empirical probability of CSP-HVDC, CSP and other dispatchable energies, such as nuclear power plants and CCS technologies is determined by cost sensitivity scenarios. Because of their low carbon emission and possible competition of dispatchability to CSP-HVDC and CSP, nuclear and CCS are considered. Hereby, each region in EUMENA is analysed separately in a modelling framework of isolated regions without grid interconnection to allow an analysis for each region separately. The analysis is performed in a "greenfield" approach. The transmission and distribution grid inside a region is considered according to [14] with specific grid values available in Table 19.

The use of an optimization model considering minimal cost as target function leads to a so-called "penny flip" effect which causes an exclusion of technologies. This exclusion can be based on minimal cost differences of technologies. To avoid this effect in the following, different cost relations of technologies are required. Table 3 shows the possible combination of cost assumptions of technologies. These cost relation combinations arise 9 different scenarios. In addition to the described sensitivity framework in Table 3, two transmission line technologies (OHL and UGC) are analysed. Consequently, the complete sensitivity includes 2 x 9 = 18 scenarios.

Table 3: Sensitivity analysis of a single technology in REMix using different technological cost relations

Cost assumption of all technologies	Cost assumption of examined technology
max_{all}	max_{tech}
	$mean_{tech}$
	min_{tech}
$mean_{all}$	max_{tech}
	$mean_{tech}$
	min_{tech}
min_{all}	max_{tech}
	$mean_{tech}$
	min_{tech}

The integration frequency or relative empirical probability of technology integration (EPTI) of these 18 scenarios is defined in Eq.(6).

$$EPTI_{18} = \frac{|EPTI_{18}| \ (capacity > 1GW)}{18} \tag{6}$$

The absolute empirical probability |EPTI| includes the integration of a technology if a minimum of 1 GW power plant capacity is reached. Base cost assumptions (max_{all}, $mean_{all}$, min_{all}) are set constant for all technologies. Only the examined technology (here: CSP-HVDC, CSP, nuclear plants, CCGT CCS and coal CCS) is calculated with each max_{tech}, $mean_{tech}$ and min_{tech} cost combination to the base cost assumptions of all other technologies. Thus, the probability of each cost assumption is assumed to be equal.

The aim of this analysis is to quantify the relative empirical probability of the above mentioned technologies in each model region. Showing also EPTI depending on CO_2 emission, two different CO_2 emission limits with 0 and 16 g CO_2/kWh_{demand} ("0 CO_2 Emission" and "Small CO_2 Emission") are used. This amounts to an overall sum of 36 (18 x 2)

scenarios. CCS technologies are excluded in the first step due to their existing CO_2 emission and incompatible comparability in this framework. In an excursion in section 3.2 CCS is included showing its EPTI (emission scenario "Small CO_2 Emission with CCS"). The small CO_2 emission limit is in the range trying to reach the below 2°C goal [15].

3   Results of the empirical probability analysis

3.1   The empirical probability of CSP-HVDC, CSP and nuclear power plants

The results in Figure 4 exhibit the integrated capacity of the analysed technologies as dots and capacity bandwidth. The boxplots show the data using quartiles. The technologies are CSP-HVDC (Figure 4a, d), CSP (Figure 4b, e) and nuclear energy (Figure 4c, f) in each model region. The spread of the bandwidth depends on the input cost assumptions and the regional resource and demand profile. Regions which are not listed e.g. in Figure 4 exclude the technology per definition. This is the case for CSP-HVDC which is only defined for EU and for CSP which is only cost efficient in MENA southern EU regions. It is recognizable that the empirical probability of CSP-HVDC and CSP increase with a lower allowed CO_2 emission limit in some model regions while the empirical probability of nuclear plants does not change (Table 4). A lower CO_2 emission limit benefits therefore the integration of CSP-HVDC and CSP. Based on the results it can be concluded that CSP-HVDC and CSP can substitute carbon emitting technologies, while in this context nuclear power does not.

Table 4: Model region average EPTI considering the CO_2 emission limit reduction from 16 to 0 g CO_2/kWh$_{demand}$

CSP-HVDC	CSP	Nuclear power plants
from 37.7% to 43.3% ▲	from 85.0% to 87.2% ▲	no change of 32.2% ◄►

The average EPTI for all model regions in Table 4 shows that an integration of CSP-HVDC is more supposable than nuclear power plants. CSP has with 85% and above the highest integration probability. An integration of CSP in MENA regions, Iberia and Turkey is therefore highly probable according to cost.

In Germany the EPTI of CSP-HVDC is 50%. An integration of this technology according to cost is therefore just as probable as improbable. The analysis of the integration probability therefore leads to the statement that CSP-HVDC can be integrated but also that it can't. Table 5 helps to clarify in more depth which cost and transmission infrastructure combinations lead to an integration of CSP-HVDC capacity in Germany and which don't. In the case of "UGC" the EPTI of CSP-HVDC is 33% whereas in the case of "OHL" the EPTI is 67%. The use of underground cable makes CSP-HVDC more expensive in relation to other

options and therefore decreases the likelihood of an integration in the cost minimizing approach. The cost combination of max_{all} and $mean_{all}$ shows that CSP-HVDC is more frequently integrated than in the cost combination min_{all}. The cost input parameters are therefore more favourable for CSP-HVDC when other energy technologies are in the same high or medium cost scenario.

Table 5: Results of cost and transmission infrastructure combination for the integration of CSP-HVDC capacity in Germany

Cost assumption of all technologies	Cost assumption of examined technology	CSP-HVDC capacity [GW] in Germany "UGC"	CSP-HVDC capacity [GW] in Germany "OHL"
max_{all}	max_{tech}	0	13
	$mean_{tech}$	59	80
	min_{tech}	98	111
$mean_{all}$	max_{tech}	0	10
	$mean_{tech}$	0	0
	min_{tech}	74	85
min_{all}	max_{tech}	0	0
	$mean_{tech}$	0	0
	min_{tech}	0	5

Capacity of CSP-HVDC is the net capacity of the power block. The colours show in green a high capacity and in yellow a small capacity.
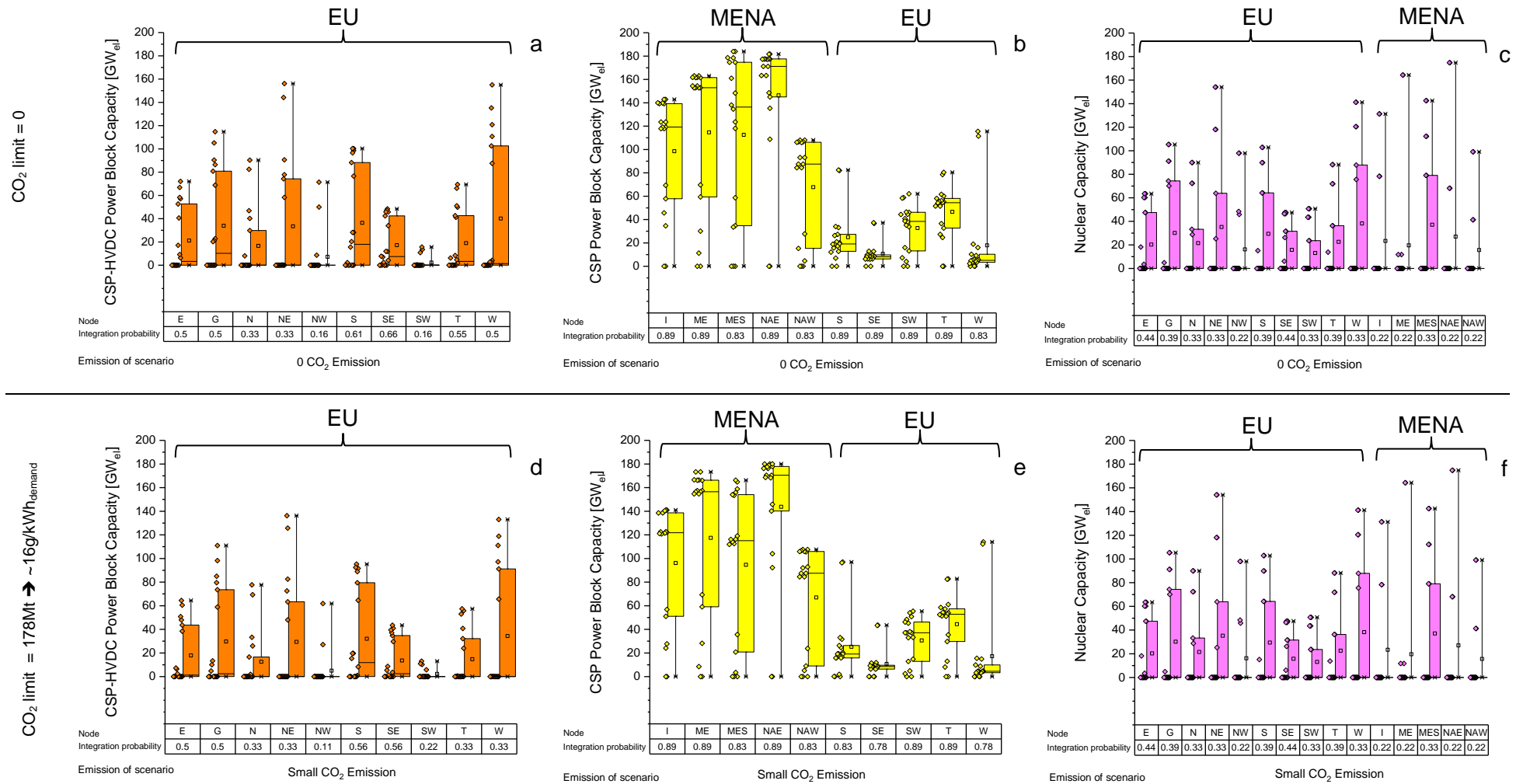
Figure 4: EPTI of CSP-HVDC, CSP and nuclear power plants – no CCS allowed

3.2 Excursion: empirical probability of CCS

In this excursion CCGT CCS and coal CCS are included, showing the EPTI in Figure 5 of CSP-HVDC (a), CSP (b), nuclear power (c), CCGT CCS (d) and coal CCS (e). Figure 5 displays the EPTI of CSP-HVDC, CSP and nuclear plants without and with CCS. The results in Figure 5 reason that the inclusion of CCS decreases the EPTI of CSP-HVDC and nuclear plants while values of CSP don't change. This leads to the conclusion that CCS may partially replace CSP-HVDC in EU, but it is still probable that CSP-HVDC may be integrated.

Table 6: Comparing average EPTI of CSP-HVDC, CSP and nuclear power plants in a scenario without CCS with a scenario allowing CCS

CSP-HVDC	CSP	nuclear power plants
from 37.7% to 35.6% ▼	no change of 85% ◄►	from 32.2% to 30.7% ▼

First values are the average EPTI in the scenario without CCS from Table 4.

The average EPTI of CCGT CCS is 50.7% and of coal CCS is 7.0%. Coal CCS is not very probable to be integrated in a low carbon energy scenario due to better alternatives. A low CO_2 emission limit leads to the use of low specific CO_2 emitting CCS technologies. An analysis of CCS technologies was also performed by [16]. In this paper lower specific CO_2 emitting CCS technologies are preferred with rising CO_2 certificate cost. CCS technologies are thus influenced by an emission limit and CO_2 cost.

Yet, it must be noted that the modelling of CCS and other technologies does not include unit commitment constraints e.g. ramping cost, minimal load and part-load behaviour or minimal downtime hours. The result is that the energy system would need more flexibility options than the model suggests. The flexibility of nuclear, coal and gas fired power plants and CCS is overestimated whereby the storage demand is underestimated [17]. In contrast, the flexibility of CSP is not underestimated because its components are designed to cover the demand flexible [18]. The EPTI of CCS is seen as non-dominant because of the missing unit commitment constraints. Thus, CCS can be neglected.
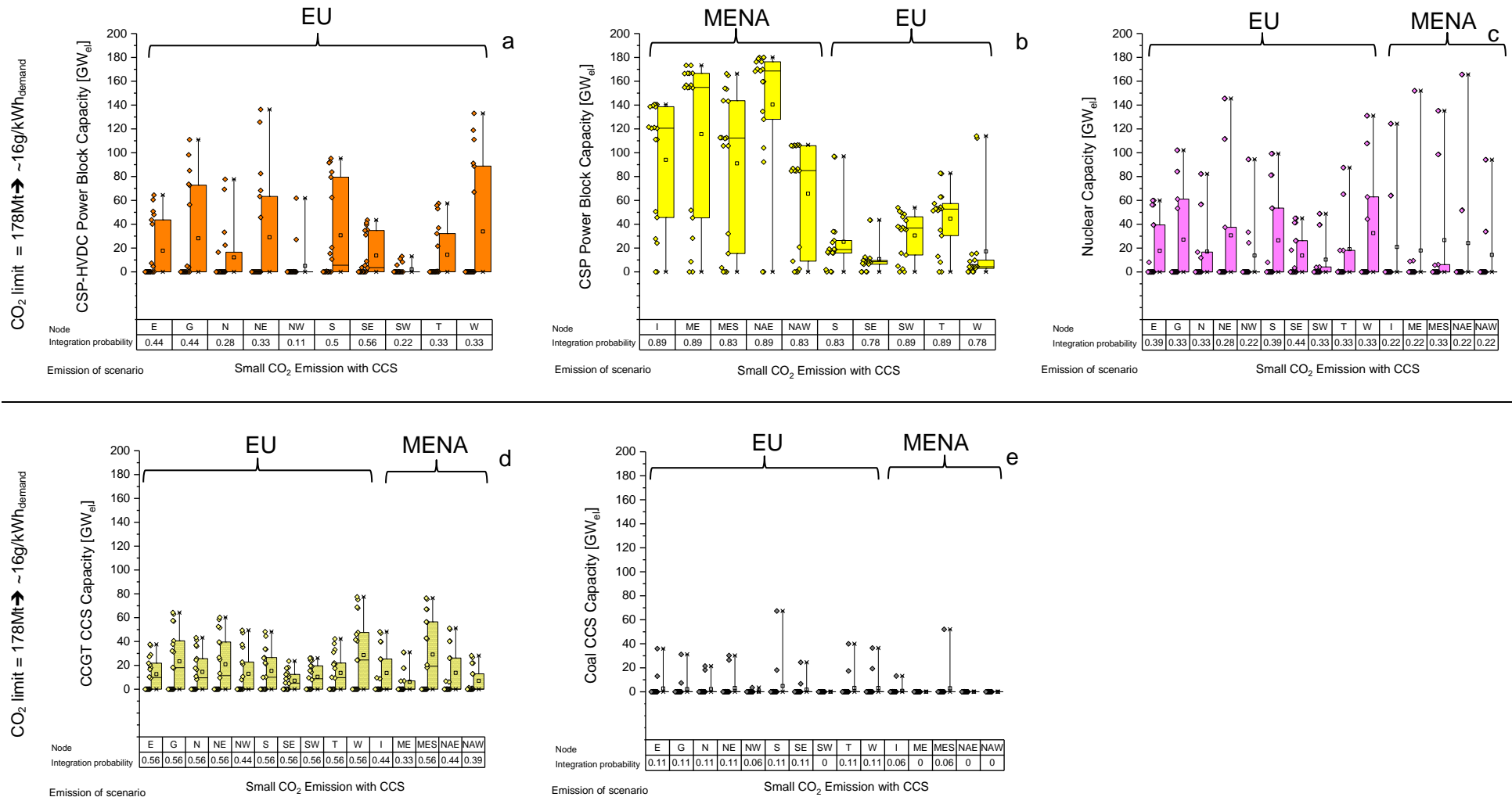
Figure 5: EPTI of CSP-HVDC, CSP, nuclear power plants, CCGT CCS, Coal CCS and the value of CCS

4   The role of CSP-HVDC and CSP for the energy system

Taking a more detailed look on CSP-HVDC and CSP, this section depicts their optimized configuration of the emission scenario "Small CO_2 Emission". The configuration criteria solar multiple (Figure 6a, b) and thermal energy storage full load hours (Figure 6c, d), are chosen to clarify the role of the technologies in the energy system and the potential differences of the cost optimal configurations of CSP-HVDC for EU, domestic CSP in MENA and domestic CSP in EU.

4.1   Solar Multiple

The solar multiple is an indicator of full load hour hours, availability and therefore also dispatchability of the renewable energy share of CSP. The higher the solar multiple the more full load hours a CSP power plant has. The solar multiple is defined as ratio of solar field capacity $P_{SF,CSP}$ and power block capacity $P_{PB,CSP}$ according to equation (7). The efficiency of the power block $\eta_{generator}$ is the product of the thermal and electrical efficiency. A solar multiple of 1 describes a system with a solar field which is large enough to provide nominal capacity for the power block under nominal irradiance (here 800 W/m^2). A solar multiple of 2 characterises a system with a solar field twice as large as with a solar multiple of 1 (with the same power block capacity). This solar field can provide energy for the power block and for a thermal storage. Thus, one solar field will directly drive the turbine while the other solar field will serve to fill the storage for night time operation [3].

$$\text{Solar Multiple:} \qquad SM = \frac{P_{SF,CSP}\ [GW_{th}]}{P_{PB,CSP}[GW_{el}] \cdot \eta_{generator}} \qquad (7)$$

Figure 6a and b shows that CSP-HVDC has a higher solar multiple than CSP. This result occurs because CSP is in competition with more cost-efficient use of PV in MENA compared to PV in EU. PV in MENA leads therefore to a reduced solar multiple of CSP in MENA in a cost-optimized framework. CSP-HVDC has with its high solar multiple a flexible base load characteristic, providing dispatchable energy according to demand.

Another effect is that CSP has a small solar multiple in southern EU regions like in **S**, **SE, T** and **W** because it is more efficient to use other technologies than building a larger solar field in such regions with a seasonal lack of DNI irradiance. The absolute configuration values of CSP in these EU regions are also comparably small. Thus, CSP can be used efficiently in southern EU but only in a small scale compared to CSP in MENA. An exception is the EU region **SW** in which the solar multiple can also achieve higher values but also comparable small values.

4.2 Thermal Energy Storage

The thermal energy storage (TES) for the analysed regions is described in Figure 6c, d with full load hours of the storage. These full load hours can be calculated according to Eq. (8) with a ration of TES capacity. $P_{TES,CSP}$ and power block capacity $P_{PB,CSP}$.

$$TES\ full\ load\ hours = \frac{P_{TES,CSP}\ [GWh_{th}]}{P_{PB,CSP}[GW_{el}]} \cdot \eta_{generator} \tag{8}$$

The results in Figure 6c reveal that the thermal energy storage of CSP-HVDC has about 13 full load hours and is thus considered as medium-term storage. The thermal energy storage of CSP has about the same range of full load hours (Figure 6d). However, CSP thermal energy storage full load hours are lower than for CSP-HVDC. The lower full load hour is attended by the lower solar multiple for CSP.
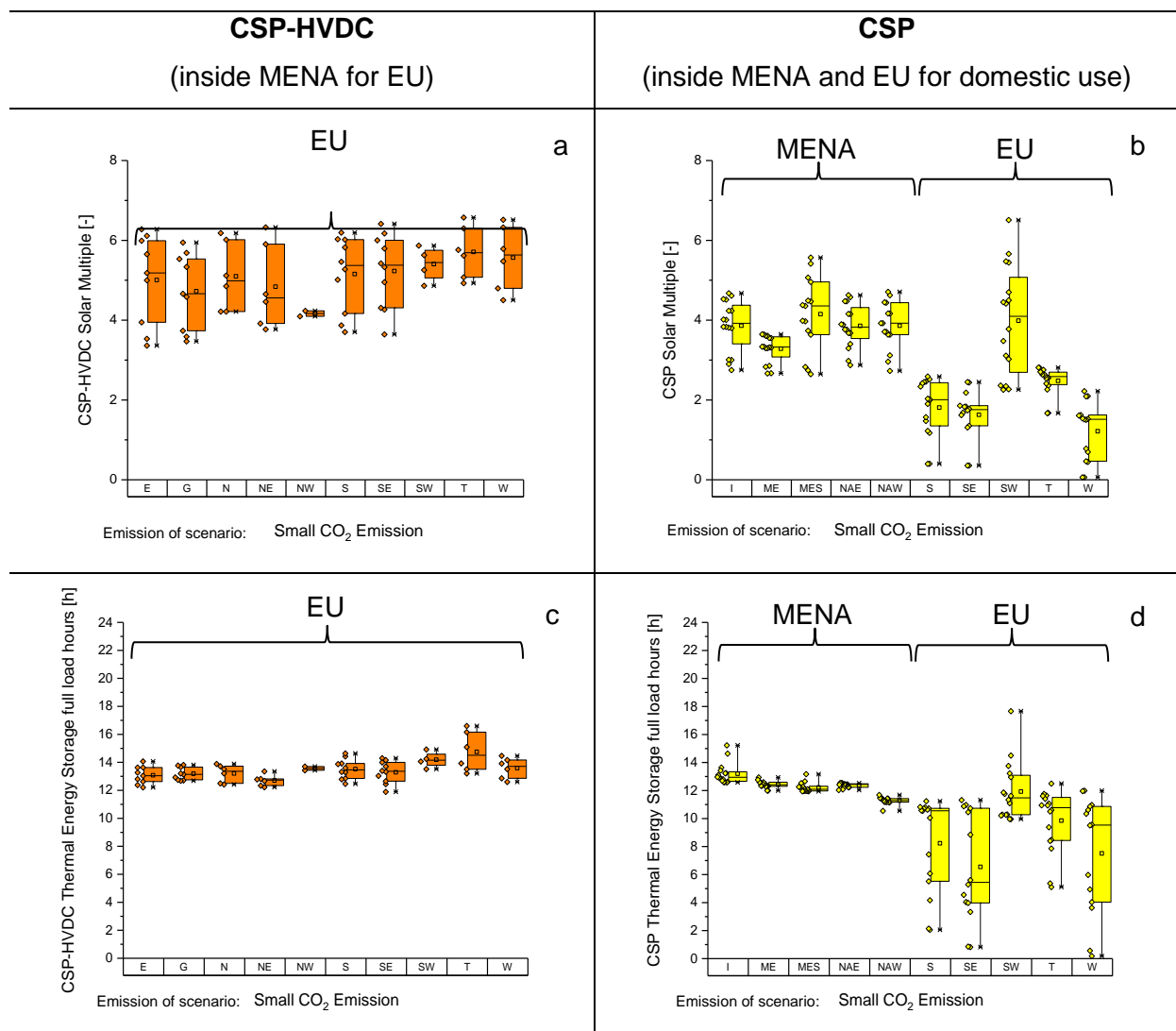

Figure 6: Solar Multiple (a, b) and Thermal Energy Storage full load hours (c, d) of CSP-HVDC (in MENA for EU) and CSP (in MENA and southern EU)

4.3   Demand for land

The demand for land of the power plant can be calculated by the solar field capacity of CSP-HVDC and CSP. Equation (9) shows how the needed area of the solar field can be calculated. This indicates how much space in desert regions is needed or in other words how much space can be used and cultivated.

$$power\ plant\ size\ [km^2] = \frac{P_{SF,CSP}\ [GW_{th}]}{0.1762} \qquad [12] \qquad (9)$$

Figure 7 reveals the resulting CSP and CSP-HVDC demand for land of the EPTI analysis in this section. The boxplots in Figure 7 show the data using quartiles. It is remarkable that the median of the demand for land of CSP-HVDC is quite similar compared to the domestic use of CSP inside the MENA region. In other words: "one mirror for MENA, one mirror for EU". However, the resulting median demand for land of CSP-HVDC is a little lower than CSP inside MENA. The median value of the demand of land for CSP inside MENA for its regional use is in the scale of the area of Switzerland (41.285 km²). The accumulation of the values for CSP inside MENA for MENA demonstrates that its median demand for land is more robust than the median value of CSP-HVDC. An accumulation of the demand for land for CSP-HVDC is visible in the under scale of the bar. Based on the large bandwidth of CSP-HVDC, a specific statement of how much area might be used for CSP-HVDC in MENA can't be done with these results.

The area of CSP inside EU for EU is comparable small with a median value of 5000 km² which equates twice the German federal state of the Saarland (2570 km²).
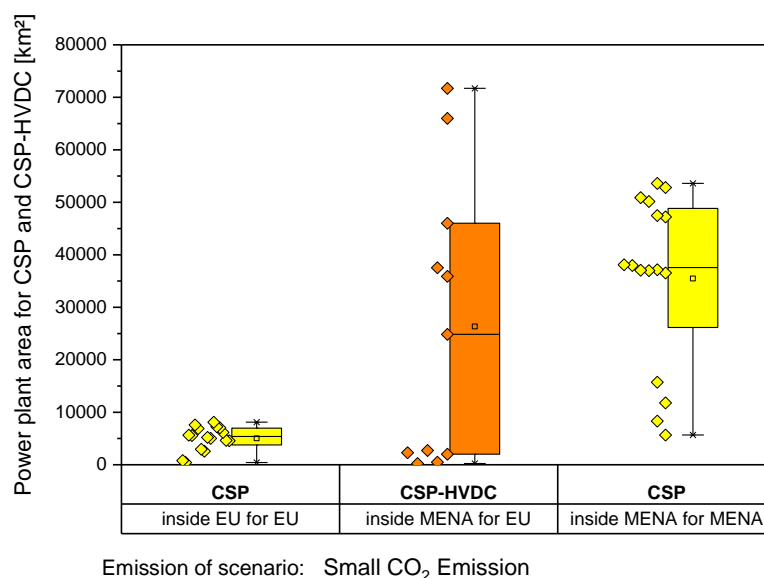

Figure 7: Bandwidth of possible area use [km²] of CSP and CSP-HVDC in EU and MENA

Table 7 supplements the configuration criteria of Figure 6 with the power block capacity, net electrical generation and the co-firing. Compared to CSP the average power block capacity and net electrical generation for CSP-HVDC are smaller. Thus, CSP in MENA has a dominant use while CSP-HVDC is more seen as a supplement for EU. Whereas CSP use a co-firing in small shares, CSP-HVDC provides energy without co-firing usage.

Table 7: CSP-HVDC and CSP configuration in sensitivity scenario of Figure 4 with small CO_2 emissions (16 g CO_2/kWh$_{demand}$)

Configuration	CSP-HVDC		CSP	
	min - max	average	min - max	average
Solar multiple [-]	3.4 - 6.6	5.1	0.1 – 6.5	3.0
Solar field size [km²]	73.7 – 12899.6	4261.9	76.3 – 13684.5	4236.8
Solar field [GW$_{th}$]	12.8 - 2272.7	751.0	13.4 - 2411.2	746.5
Thermal energy storage full load hours [h]	11.9 – 16.6	13.4	0.2 – 17.7	10.6
Thermal energy storage [GWh$_{th}$]	41.8 - 5091.6	1854.6	55.4 - 6044.4	2366.9
Power block capacity [GW]	1.3 - 136.3	50.5	1.9 – 180.0	76.1
Net electrical generation [TWh/y]	7.5 - 842.9	321.7	9.0 - 1256.2	444.3
Co-firing with natural gas [TWh/y]	0	-	0.2 - 20.5	3.6

Average values are calculated considering all regions equally. The values (in grey) reflect the relative configuration of the power plants. The other values show the absolute dimension in a possible bandwidth.

Detailed regional configuration values of CSP-HVDC and CSP with the frame conditions of 0 and 16 g CO_2/kWh$_{demand}$ also with CCS are shown in the appendix Figure 28 to Figure 31.

5   Conclusion, suggestion for improvements and outlook

In this paper the empirical probability of CSP-HVDC, CSP, nuclear power and CCS are introduced. It can be concluded that the empirical probability of CSP-HVDC implies a possible integration of this technology. It should be noted that the cost assumptions of CSP

and the pathway of HVDC are assumed as relative conservative and that CSP still renders a cost reduction till 2050 due to its advancing learning curve. Therefore CSP-HVDC is rather underestimated than overrated and it has therefore a high potential to be integrated. Nuclear plants and CCS are also possibly integrated yet with a lower EPTI of nuclear plants than CSP-HVDC or under the very optimistic modelling conditions for CCS.

The results are achieved using a simplified technological model. A detailed technological CSP model regarding the resulting configuration is needed. Modelling improvements can consider a higher spatio-temporal resolution showing more details. Other energy system evaluation criteria such as infrastructural need, curtailment, grid stress are important to show the value of CSP-HVDC for a holistic energy system analysis. The model doesn't consider scale effects such as higher internal demand with a rising solar multiple so-called parasitic losses. A combination of CSP and PV may attenuate such losses with the use of cost-efficient PV. The use of the thermal storage as a medium term storage by the entire energy system can be also a promising possibility for CSP because surplus electricity of the system can be stored in the thermal storage of CSP to avoid otherwise higher electrical storage capacity and curtailment of the energy system. The high solar multiple of CSP-HVDC (4-6) leads to potential constructional questions especially regarding parasitics in a large solar field size. Transforming desert areas in arable land raises the question which of the CSP technologies (tower, trough or Fresnel) is favourable to be used for this purpose and at the same time efficient for an export via HVDC. Conceptual technological alternatives to CSP-HVDC have a low technology readiness level such as Wind or PV combined with a thermal/electrical storage, heat pump and co-firing option, or nuclear fusion and are therefore intangible. Technological breakthroughs are uncertain from today's point of view. Such technological concepts are important for further research activities but should be definitely no obstacles to concretise technically functioning CSP-HVDC reaching climate protection targets as soon as possible.

As a result of the configuration values of CSP-HVDC and CSP it is concluded that the two technologies fulfil different roles in the analysed regions. CSP-HVDC has a high solar multiple and a base load characteristic. CSP in MENA has a lower solar multiple due to efficient combination of CSP and PV in the domestic energy mix. Based on comparable high thermal energy storage full load hours, the medium-term thermal storage of CSP in MENA is frequented like in the CSP-HVDC configuration. Thus, CSP in MENA has also a baseload characteristic but a lower use of the solar field than CSP-HVDC. The CSP power plants in the EU for domestic use have a lower solar multiple and lower thermal energy storage full

load hours due to other more efficient technologies and the drastic reduction of DNI in winter. CSP in EU for domestic use shows therefore a commitment to medium load levels.

It is remarkable that the median of the demand for land of CSP-HVDC is quite similar compared to the domestic use of CSP inside the MENA region. In other words: "one mirror for MENA, one mirror for EU". Thus, CSP power plants can be built hand in hand for the domestic use in MENA and with separate power plants for an export to EU.

Abbreviations

CCGT	Combined cycle gas turbine
CCS	Carbon capture and storage
CSP	Concentrating Solar Power
CSP-HVDC	Concentrating solar power with point-to-point high voltage direct current line
DC	Direct Current
EPTI	relative Empirical Probability of Technological Integration
EU	geographical Europe
EUMENA	Europe, Middle East and North Africa
HVDC	high voltage direct current line
max, mean, min	Cost sensitivities
ME	Middle East
NA	North Africa
O&M	Operation and maintenance cost
OHL	Overhead Line
P2P	Point-to-Point transmission line
PV	Photovoltaic
REMix-EnDAT	Renewable Energy Mix Energy Data Analysis Tool
REMix-OptiMo	Renewable Energy Mix Optimization Model
UGC	Underground Cable

Parameters

$c_{Emission}$	[k€/GWh]	specific emission cost
c_{Fuel}	[k€/GWh]	specific fuel cost
$c_{O\&M\,Fix}$	[%/y]	specific operation and maintenance fix costs
$c_{specInv}$	[k€/MW]	specific investment cost
ep_{18}	[-]	relative empirical probability using 18 scenarios
EP_{18}	[-]	absolute empirical probability using 18 scenarios
$f_{annuity}$	[-]	Annuity factor
i	[%]	Interest and discount rate
$P_{existCap}$	[GW$_{el}$]	Capacity of existing power plants
$P_{HVDC,\,gross}$	[GW$_{el}$]	Gross capacity of the HVDC transmission line
$P_{PB,\,CSP}$	[GW$_{el}$]	Capacity of the CSP power block
$P_{SF,\,CSP}$	[GW$_{th}$]	Capacity of the CSP solar field
$P_{TES,\,CSP}$	[GWh$_{th}$]	Thermal energy storage capacity of the CSP
$\eta_{generator}$	[%]	Efficiency of the generator as product of the thermal and electrical efficiency
η_{charge}	[%]	Charging efficiency of the storage
$\eta_{discharge}$	[%]	Discharging efficiency of the storage
η_{self}	[%/h]	Self-discharging rate of the storage per hour
$s_{gen}(t)$	[-]	Normalised generation time series of fluctuating energy
SM	[-]	Solar Multiple
Δt	[h]	Calculation time interval
t_y	[y]	Amortization time
y	[year]	year

Variables

$C_{capital}$	[k€/y]	Annual depreciation of capital expenditure
$C_{operation}$	[k€/y]	Annual operation and maintenance costs
$P_{addedCap}$	[GW$_{el}$]	Capacity of additional power plants
$P_{gen}(t)$	[GW$_{el}$]	Power generation
$Q_{addedCap}(t)$	[GW$_{th}$]	Capacity of model endogenous CSP solar field
$Q_{BUS}(t)$	[GW$_{th}$]	Thermal output of the CSP co-firing system
$Q_{charge}(t)$	[GW$_{th}$]	Thermal energy storage input
$Q_{curtail}(t)$	[GW$_{th}$]	Thermal curtailment of the solar field
$Q_{disharge}(t)$	[GW$_{th}$]	Thermal energy storage output
$Q_{SF}(t)$	[GW$_{th}$]	Thermal output of the solar field
$U_{level}(t)$	[GWh$_{th}$]	Thermal energy storage level

6   Acknowledgement

7   References

[1] DLR, "Concentrating Solar Power for the Mediterranean Region (Med-CSP)," 2005.

[2] DLR, "Trans-Mediterranean interconnection for Concentrating Solar Power (TRANS-CSP)," 2006.

[3] F. Trieb, C. Schillings, T. Pregger and M. O'Sullivan, "Solar electricity imports from the Middle East and North Africa to Europe," *Energy Policy,* vol. 42, 2012.

[4] BETTER, "Bringing Europe and Third countries closer together through renewable Energies," 2015.

[5] P. Gauché, J. Rudman, M. Mabaso, W. A. Landman, T. W. v. Backström and A. C. Brent, "System value and progress of CSP," *Solar Energy,* vol. 152, pp. 106-139, 2017.

[6] F. Trieb, T. Fichter and M. Moser, "Concentrating solar power in a sustainable future electricity mix," *Sustainability Science,* vol. 9, p. 47–60, 2014.

[7] S. Pfenninger, P. Gauché, J. Lilliestam, K. Damerau, F. Wagner and A. Patt, "Potential for concentrating solar power to provide baseload and dispatchable power," *Nature Climate Change,* vol. 4, p. 689–692, 2014.

[8] IRENA, "Planning for the Renewable Future: Long-term modelling and tools to expand variable renewable power in emerging economies," International Renewable Energy Agency, Abu Dhabi, 2017.

[9] G. Knies and A. Bennouna, "Nordafrikanisch - Europäischer Solarenergie Verbund. Workshop des Hamburger Klimaschutz-Fonds HKF am 9.4. 1997 an der TU Hamburg Harburg," 1997.

[10] United Nations, "World Population Prospects: The 2015 Revision," 2015.

[11] Y. Scholz, Renewable energy based electricity supply at low costs : development of the REMix model and application for Europe, Stuttgart: University Library of the University of Stuttgart, 2012.

[12] D. Stetter, Enhancement of the REMix energy system model : global renewable energy potentials, optimized power plant siting and scenario validation, Stuttgart: University Library of the University of Stuttgart, 2012.

[13] H. Gils, Y. Scholz, T. Pregger and D. Luca de Tena, "Integrated modelling of variable renewable energy-based power supply in Europe," *Energy,* vol. 123, p. 173–188, 2017.

[14] D. Hess, M. Wetzel and K.-K. Cao, "Representing node-internal transmission and distribution grids in energy system models," *Renewable Energy,* 2018.

[15] J. Rogelj, G. Luderer, R. C. Pietzcker, E. Kriegler, M. Schaeffer, V. Krey and K. Riahi, "Energy system transformations for limiting end-of-century warming to below 1.5 °C," *Nature Climate Change,* vol. 5, p. 519–527, 2015.

[16] Y. Scholz, H. C. Gils and R. C. Pietzcker, "Application of a high-detail energy system model to derive power sector characteristics at high wind and solar shares," *Energy Economics,* vol. 64, pp. 568-582, 2017.

[17] F. Cebulla and T. Fichter, "Merit order or unit-commitment: How does thermal power plant modeling affect storage demand in energy system models?," *Renewable Energy,* vol. 105, pp. 117-132, 2017.

[18] T. Fichter, Long-term Capacity Expansion Planning with Variable Renewable Energies - Enhancement of the REMix Energy System Modelling Framework, Stuttgart: Universität Stuttgart, 2017.

[19] IEA, "International Energy Agency Statistics," 2017. [Online]. Available: http://www.iea.org/statistics/. [Accessed 14 02 2015].

[20] F. Trieb and U. Klann, "Modeling the Future Electricity Demand of Europe, Middle East and North Africa," Stuttgart, 2006.

[21] IPCC, "Mitigation of Climate Change," 2014.

[22] IPCC, "Mitigation of Climate Change," 2014.

[23] IIASA, "Shared Socioeconomic Pathways Database," 03 2013. [Online]. [Accessed 03 08 2015].

[24] L. Gruber, "Synthese globaler, elektrischer Lastganglinien," Berlin, 2012.

[25] G. Pleßmann, M. Erdmann, M. Hlusiak and C. Breyer, "Global Energy Storage Demand for a 100% Renewable Electricity Supply," *Energy Procedia,* vol. 46, pp. 22-31, 2014.

[26] S. Kühnel, Investigation of the variability of solar and wind electricity generation potentials in Europe and North Africa, Oldenburg: Karl von Ossietzky University, 2013.

[27] H. Gils, "Economic Potential for Future Demand Response in Germany – Modelling Approach and Case Study. doi:10.1016/j.apenergy.2015.10.083," *Applied Energy,* vol. 162, p. 401–415, 2016.

[28] H. Gils, "Assessment of the theoretical demand response potential in Europe. doi:10.1016/j.energy.2014.02.019," *Energy,* vol. 67, pp. 1-18, 2014.

[29] N. May, "Eco-balance of a Solar Electricity Transmission from North Africa to Europe," Braunschweig, 2005.

[30] G.-G. Marcos and L.-A. Roberto, "Assessment of the European potential for pumped hydropower energy storage: A GIS-based assessment of pumped hydropower storage potential," 2013.

[31] A. Moser, "Unterstützung der Energiewende in Deutschland durch einen Pumpspeicherausbau," 2014.

[32] FIAS, 2017. [Online]. Available: https://github.com/FRESNA/powerplantmatching. [Accessed 03 05 2016].

[33] R. Jung, S. Röhling, N. Ochmann, S. Rogge, R. Schellschmidt, R. Schulz and T. Thielemann, "Abschätzung des technischen Potenzials der geothermischen Stromerzeugung und der geothermischen Kraft-Wärmekopplung (KWK) in Deutschland," 2002.

[34] M. Tum, I. M. Kurt P. Günther, G. Kindermann and E. Schmid, "Sustainable Bioenergy Potentials for Europe and the Globe," *Geoinformatics & Geostatistics: An Overview,* pp. 1-10, 2013.

[35] IEA, "Technology Roadmap: Solar Photovoltaic Energy," 2010.

[36] IEA, "Data from Market Allocation (MARKAL) model, International Energy Agency and Brookhaven National Laboratory," 2009.

[37] OPENEI NREL, "The data below was downloaded from the Transparent Cost Database at http://en.openei.org/apps/TCDB/".

[38] Environmental Protection Agency, *Data from Integrated Power Model (IPM), ICF International.,* 2010.

[39] IRENA, "IRENA Hydro Power," 2012. [Online]. Available: http://www.irena.org/documentdownloads/publications/re_technologies_cost_analysis-hydropower.pdf.

[40] J. Nitsch and et al., "Long-term scenarios and strategies for the deployment of

renewable energies in Germany in view of European and global developments," 2012.

[41] Pregger, "Vergleichende Bewertung der Integration einer zentralen versus einer dezentralen Wasserstofferzeugung in die zukünftige Stromversorgung Deutschlands," 2015.

[42] U. Albrecht, M. Altmann, J. Michalski, T. Raksha and W. Weindorf, "Analyse der Kosten erneuerbarer Gase," BWE, 2013.

[43] D. Fürstenwerth and et al., "Stromspeicher in der Energiewende," Agora, 2014.

[44] J. Nitsch and T. Pregger, "Kostenbilanz des Ausbaus erneuerbarer Energien in der Stromerzeugung bei unterschiedlichen Preisbildungen am Strommarkt," *Vierteljahrshefte zur Wirtschaftsföderung,* vol. 82, pp. 45-59, 2013.

[45] E. S. Rubin, C. Chen and A. B. Rao, "Cost and performance of fossil fuel power plants with CO2 capture and storage," *Energy Policy,* vol. 35, p. 4444–4454, 2007.

[46] European Commission, "Press releases database," 08 10 2014. [Online]. Available: http://europa.eu/rapid/press-release_IP-14-1093_de.htm. [Accessed 20 03 2015].

[47] G. v. Goerne, CO2-Abscheidung und -Lagerung(CCS) in Deutschland, Germanwatch Nord-Süd Initiative e.V., 2009.

[48] H. Brakelmann, "Netzverstärkungs-Trassen zur Übertragung von Windenergie: Freileitung oder Kabel ?," Rheinberg, 2004.

[49] D. Hess, FERNÜBERTRAGUNG REGELBARER SOLARENERGIE VON NORDAFRIKA NACH MITTELEUROPA, Stuttgart: University Library of the University of Stuttgart, 2013.

[50] L. Neij, "Cost development of future technologies for power generation—A study based on experience curves and complementary bottom-up assessments," *Energy Policy 36,* p. 2200– 2211, 2008.

[51] CSP-Today, "CSP-Today," 15 02 2016. [Online]. Available: http://www.csptoday.com/.

[52] P. Viehbahn and et al., "EU-NEEDS scenario pesimistic," 2008.

[53] Greenpeace, "Global Concentrating Solar Power Outlook (scenario optimistic)," 2009.

8   Appendix

8.1   Basic modelling assumptions

8.1.1   Supply technologies

The REMix model includes weather dependent technologies such as photovoltaic, wind onshore, wind offshore and hydro run-of-river so-called fluctuating renewable energies and non-weather dependent technologies such as biomass, geothermal energy, nuclear, gas, coal fired power plants (also CCS) and CSP with co-firing so-called dispatchable energies. Biomass, geothermal and CSP with thermal energy storage and co-firing are defined as renewable dispatchable technologies. Dispatchable energies can provide electricity according to the demand and offer firm capacity. The electricity generating renewable technologies applied in the paper are listed in Table 8. These technologies are available today and they are functioning. Contrarily, technologies with a low technological readiness level such as nuclear fusion or a hydrogen turbine are not considered. This allows a pragmatic and robust energy system analysis without speculation of technological breakthroughs from today's point of view. Non-renewable technologies such as nuclear, gas, coal fired power plants (also CCS) are characterised in Table 14 on page 60. Defining the characteristic of a technology, a representative example out of a technology group is selected, but not the whole bandwidth of all specific occurrences of one technology is examined. The examples are representative for the general characteristic of a chosen technology. However, a simplification makes sense comparing only the technology groups in competition to each other. Other applied technologies defined as flexibility options such as electrical storages and the electrical grid. Potentials of pump storage, hydro run-of-river, hydro reservoir, geothermal energy, solid biomass and CSP are limited and are made available in the appendix Table 10.

Table 8: Classification and characteristic of used renewable energies for electricity generation based on [11] – hydro reservoir is considered neither as fluctuating nor as dispatchable but as long term storage with additional natural inflow.

Technology class of electricity generating power plants		Characteristics	Range of validity
Fluctuating renewable energies	Photovoltaic	Silicon cells with a module efficiency of 18%	Standard test conditions: 25 °C module temperature, 1000 W/m^2 irradiance
	Wind Onshore	Rotor diameter: 130 m Hub height: 132 m	Start-up wind speed: 2 m/s, nominal power output is reached at 12 m/s. Cut-off was set to start at 25 m/s and to end at 35 m/s.
	Wind Offshore	Rotor diameter: 140 m Hub height: 192 m	
	Hydro run-of-river (here fluctuating because of fluctuating water level and no co-firing option)	No power plant model – analysis is based on empirical time series	Power plants in operation, annual generation and generation potentials in Germany
Dispatchable renewable energies (with co-firing option)	Biomass	Power plant with steam turbine - 35% electric efficiency - using forest wood, waste wood, straw and energy crops	Domestic share of net primary production potential, yields and competing use scenarios per country for forestry, agriculture and other sectors - agricultural statistics.
	Geothermal power	Enhanced geothermal system (EGS)	Depth range 2000 - 5000 m
	Concentrating Solar power	Parabolic trough power plant with molten salt storage - 37% power block efficiency and 95% storage efficiency -	Reference irradiance - direct normal irradiance (DNI) - with 800 W/m^2, tracking the sun along the north south axis

Other characteristic of power plant and storage are available with technological an economic data in Table 12 to Table 16.

8.1.2 Demand model

The analysis considers only the electricity demand. However, the demand model includes an electricity share of heat and mobility. The occurring electricity demand of these two sectors is added to the conventional electricity demand. In the following the assumptions of the demand until the year 2050 are explained showing the data that build the basis of the assumption in the demand model. The historical data of electricity, heat and mobility in the used model start in the year 2010 and are taken form IEA database [19].

- Electricity: net electricity demand (electricity, final consumption)
- Heat: residential and commercial heat demand (from coal, oil and gas)
- Mobility: transport demand (from oil)

The development of the electricity sector is derived from the GDP according to DLR [20]. This reference uses a scenario for the development of the GDP per capita growth rate. The used GDP per capita growth rate in the scenario "closing the gap" assumes to reduce the difference of GDP per capita of a given country to 50% compared with the GDP per capita of the USA in the year 2050. Population data are taken from the UN medium scenario [10]. For the development of the electricity share of the heat sector a 60% electricity share of global buildings final energy demand until 2050 is used and a demand reduction per capita and year (2010 to 2050) of 0.65% in OECD, 0.39% in Middle East and Africa and 0.28% in Eastern Europe and Russia is assumed [21]. The conversion factor using final energy of heat from oil, gas or coal is 90%. For the development of the electricity share of the mobility sector outgoing from 2020 a 15% electricity share of final energy demand until 2050 is used and a demand reduction per capita and year (2010 to 2050) of 1.08% in OECD, -0.45% in Middle East and Africa and -0.82% in reforming countries is assumed [22], [23]. The conversion factor using final energy from oil for mobility is 30%. For heat and mobility there is still a higher share of carbon resource than in the electricity sector in 2050. However, the assumption considers low carbon emission trying to reach the 2°C target [15].

The resulting electricity demand in Table 9 of heat and mobility is added to the electrical load curve with the same profile because today's load curve already includes heat and mobility shares. The hourly profile of the electrical load curve is taken from ENTSO-e in 2006, Arab Union of Electricity (AUE) in 2012 and a synthetic load profile from [24], [25] and thus represent historical demand curve. It is assumed that these load curves do not have another characteristic than in the year 2050.

Table 9: Annual electrical demand of electricity, heat and mobility sector in 2010 and 2050

Model region	Electricity demand [TWh]		Electrical heat demand [TWh]*	Electrical mobility demand [TWh]*	Total electrical demand [TWh]	
year	2010	2050	2050	2050	2010	2050
G	532	510	173	22	532	706
N	382	541	13	17	382	571
E	235	337	82	11	235	429
S	436	522	141	27	436	689
W	641	673	205	42	641	920
NW	370	552	201	32	370	785
NE	608	839	170	27	608	1037
SE	195	298	15	8	195	321
NAE	151	1127	19	31	151	1178
NAW	71	582	74	19	71	674
SW	295	315	9	18	295	342
T	175	509	90	14	175	613
MES	150	796	99	56	150	950
I	186	484	362	28	186	874
ME	393	869	18	87	393	974
Sum	4819	8953	1672	439	4819	11064

*Additional electrical heat and mobility demand are assumed to be 0 in the year 2010.

The rising electrical demand in EUMENA, which more than doubles from 4819 TWh in 2010 to 11064 TWh in 2050, leads to a capacity expansion and higher demand of resources. Thus, in Europe dispatchable renewable energies such as biomass and geothermal energy can reach their techno-economic limit. Solving this lack, Wind, PV, storage and CSP inside Europe and from MENA can provide renewable energy. It can be expected that a rising electrical demand may lead to a rising demand of renewable dispatchable energy and therefore to a rising demand of a transfer of CSP generated electricity from MENA to Europe.

8.1.3 Technological time series and electrical load curve

The time series of CSP, photovoltaic, wind onshore, wind offshore, hydro run-of-river power plants and hydro reservoir natural inflow are country-wide averages calculated with REMix-EnDAT based on bottom-up power plant models (see Table 8) [11], [12]. This calculation includes exclusion areas for renewable energies which define with technology parameters the potential of each renewable energy technology. For each grid box, the approach yields

hourly power generation based on technology parameters and resource availability. The hourly time series are available of the years 1984-2004 on global level (resolution 0.045° x 0.045° or ~50km x 50km at equator) [12] and of the years 2006 - today on European level (resolution 0.083° x 0.083°, ~10km x 10km) [11]. For the analysis a typical meteorological year is considered, which is the year 2006 in Europe [11] and the year 2002 in MENA [12]. Two different years can be chosen due to relative low meteorological differences. On European level the output of the time series deviate in the available years of about 15% max. [26]. Possible changes of the renewable resource availability due to climate change are an uncertainty which is not considered in the analysis. Peak load of demand and average resource full load hours of the model regions are available in Table 11. These input data are important for a reproducibility of the results showing key characteristics of annual input values as well as temporal intensity and temporal availability. Figure 8 serves as an example of the electrical load and technological time series of one year for Germany (country average). Here isopleth diagrams are used to illustrate such time series over the day of the year (y-axis) and over the hour of the day series (x-axis). They show in (a) the electrical load as share of peak load, in (b) the normalised availability of generated electricity by PV capacity, in (c) by wind turbines offshore, in (d) by wind turbines onshore, in (e) by hydro run of river power plants, in (f) the normalised availability of natural inflow by hydro reservoir power plants, in (g) by imports of hydro reservoir power plants from Norway, in (h) the normalised availability of generated thermal energy by the solar field of CSP in MENA for Germany and are related to the design point of 800 W/m^2. The hydro reservoir time series are derived from hydro run of river [11]. The CSP time series is an average of selected CSP hotspots.

The temporal profiles reveal the intensity and availability of the demand and the resources. Characteristic for the time series is the time period of regularly and unregularly low and high availability. For example the wind resources show irregular monthly and seasonal lacks (green colour Figure 8c, d) of wind compared to solar resources (black in Figure 8b,h). Solar resources are more periodical available during a year than wind or hydro resources. The availability of the solar resources PV (GHI) is smoother than the scattered resource of CSP (DNI). Comparing PV in Germany and CSP in MENA, it is visible that in winter PV drops in Germany while CSP in MENA stays in its availability nearly constant. Hydro time series are seasonally less fluctuating than wind or solar but not always such intensively available. The load curve shows a peak demand in winter which is typical in northern European regions. All isopleth diagrams of the used model regions refer to one year, start in the lower left corner (0,0) on January 1st and are shown in Figure 8 to Figure 22.

Europe:
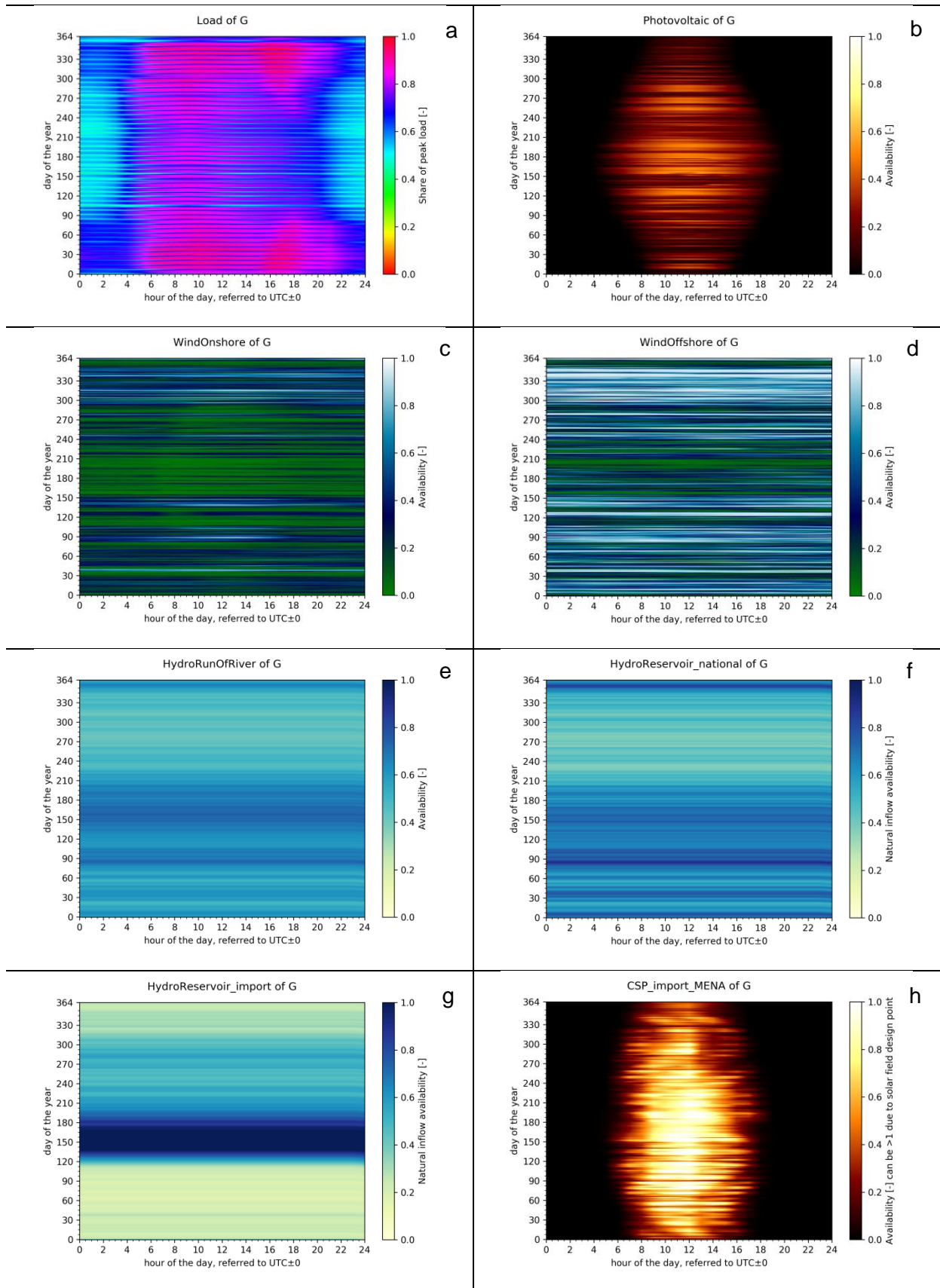
Figure 8: Load and technological time series of model region G
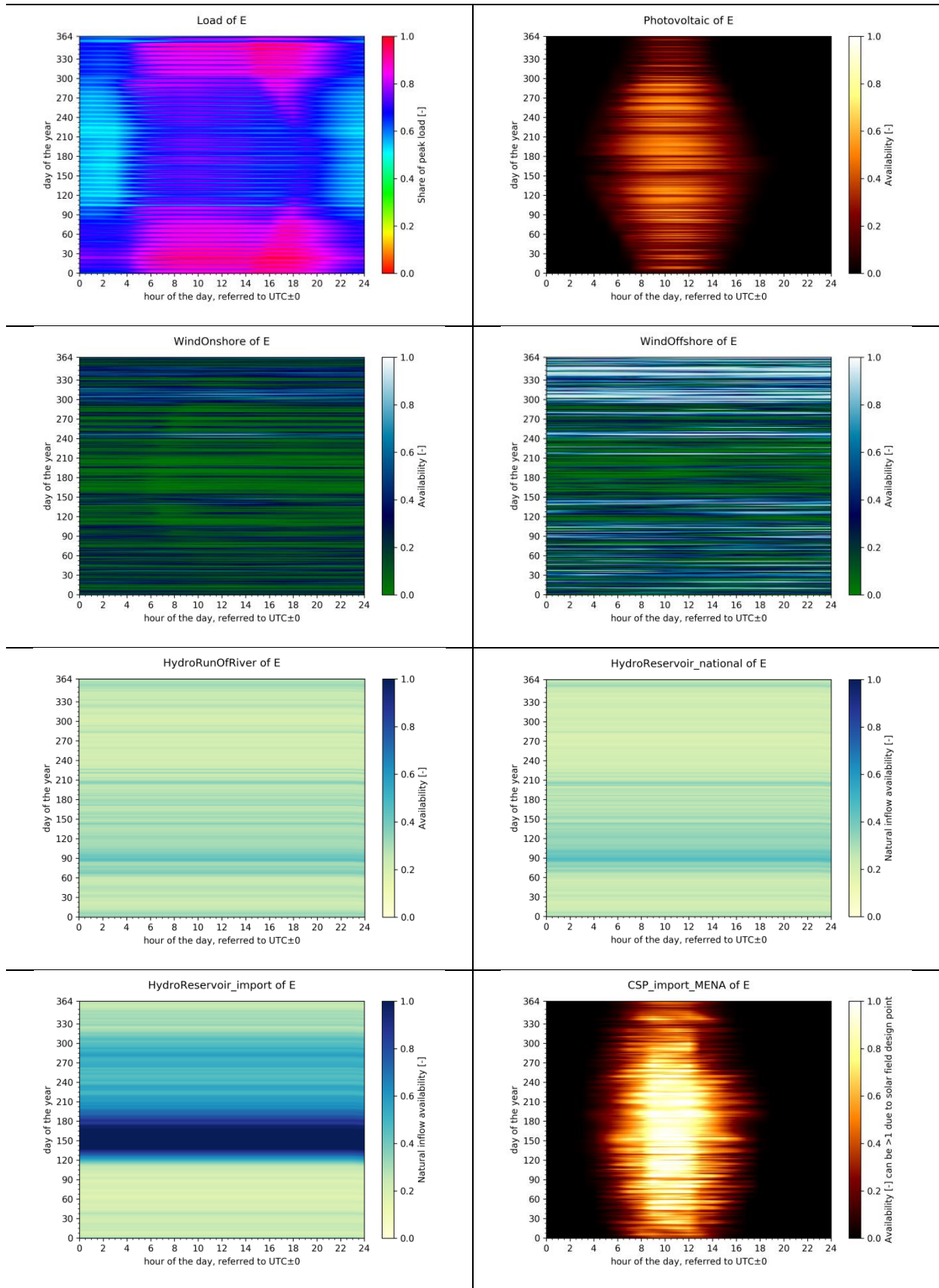
Figure 9: Load and technological time series of model region E
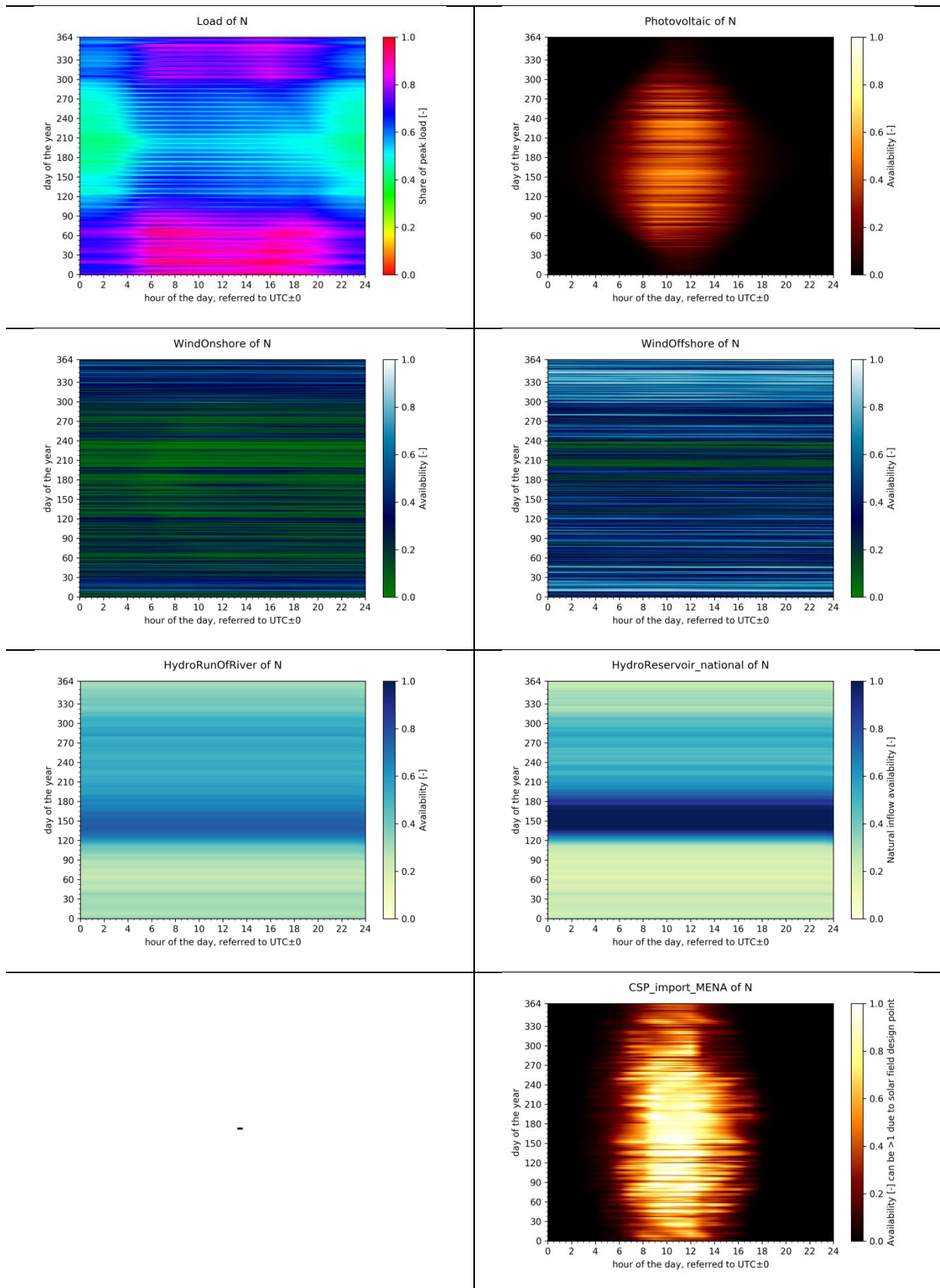
Figure 10: Load and technological time series of model region N
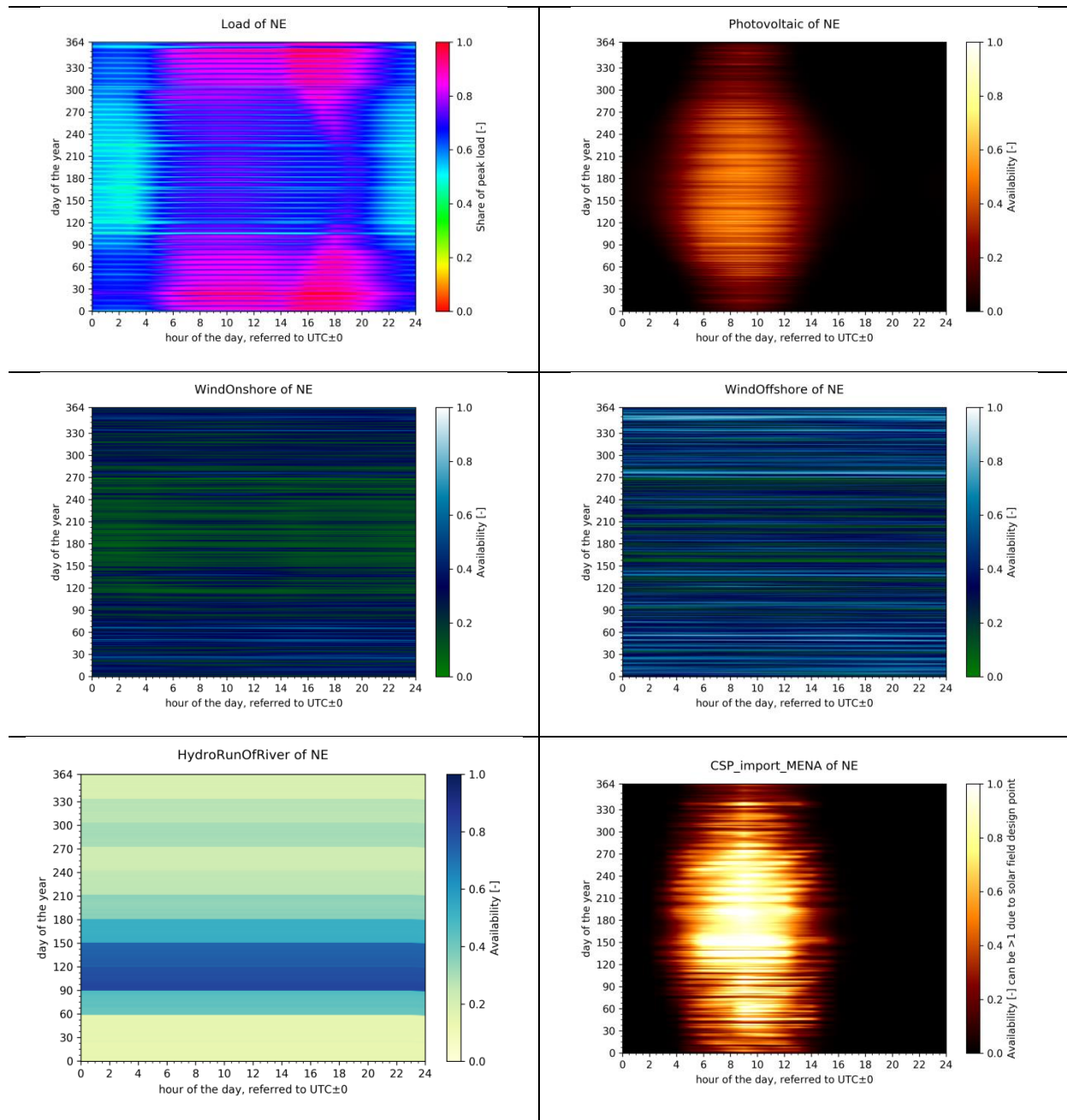
Figure 11: Load and technological time series of model region NE
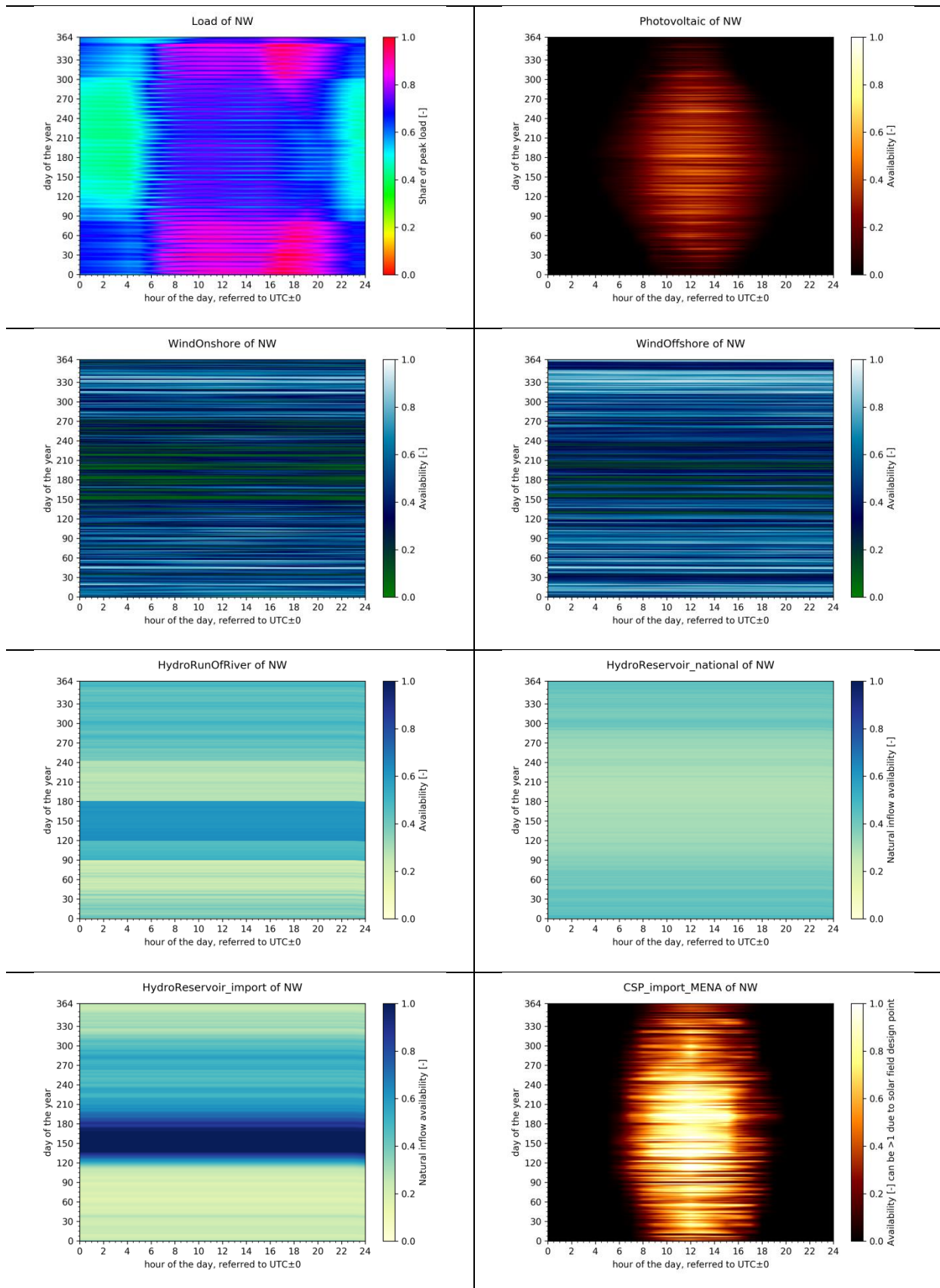
Figure 12: Load and technological time series of model region NW
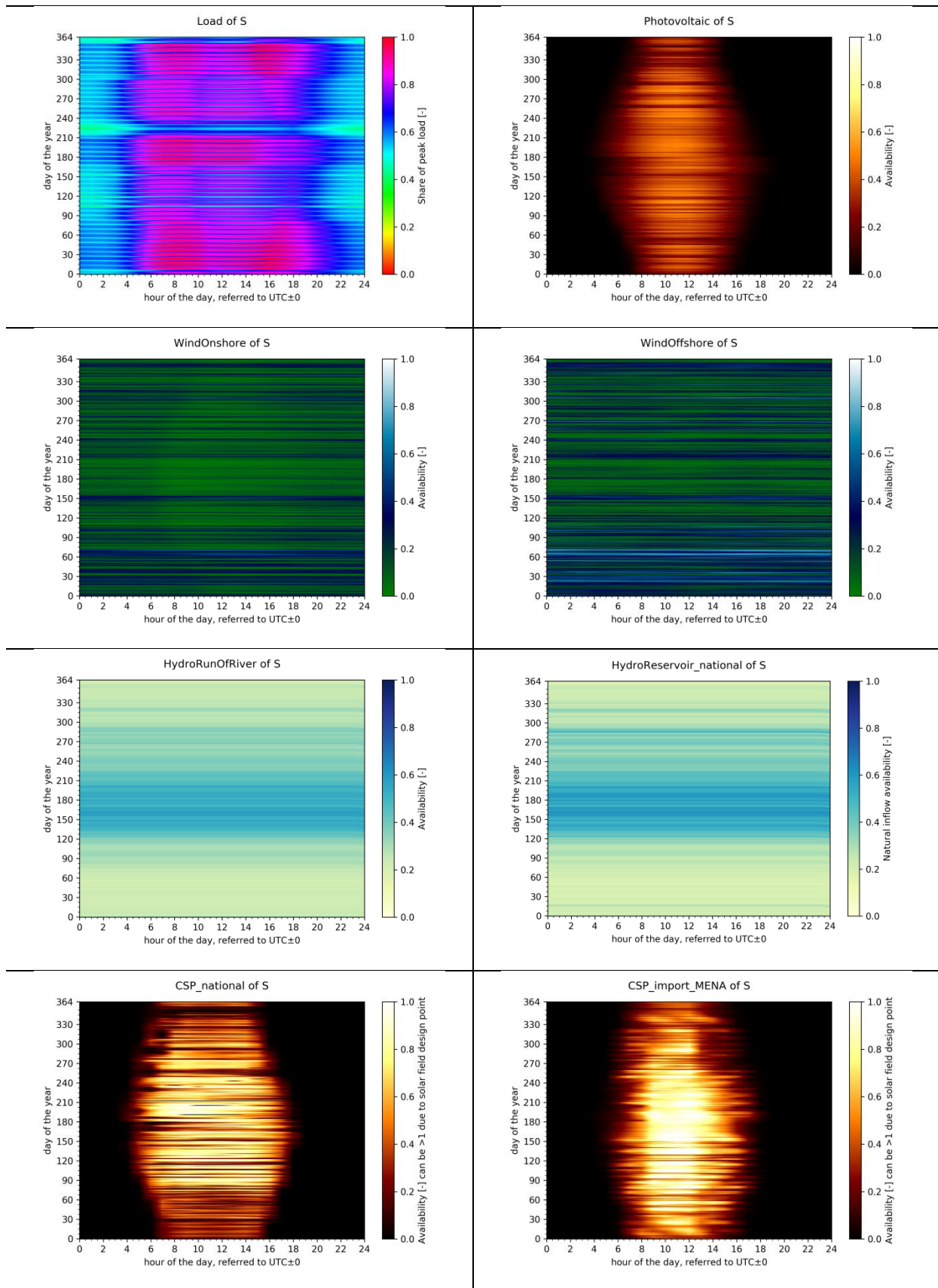
Figure 13: Load and technological time series of model region S
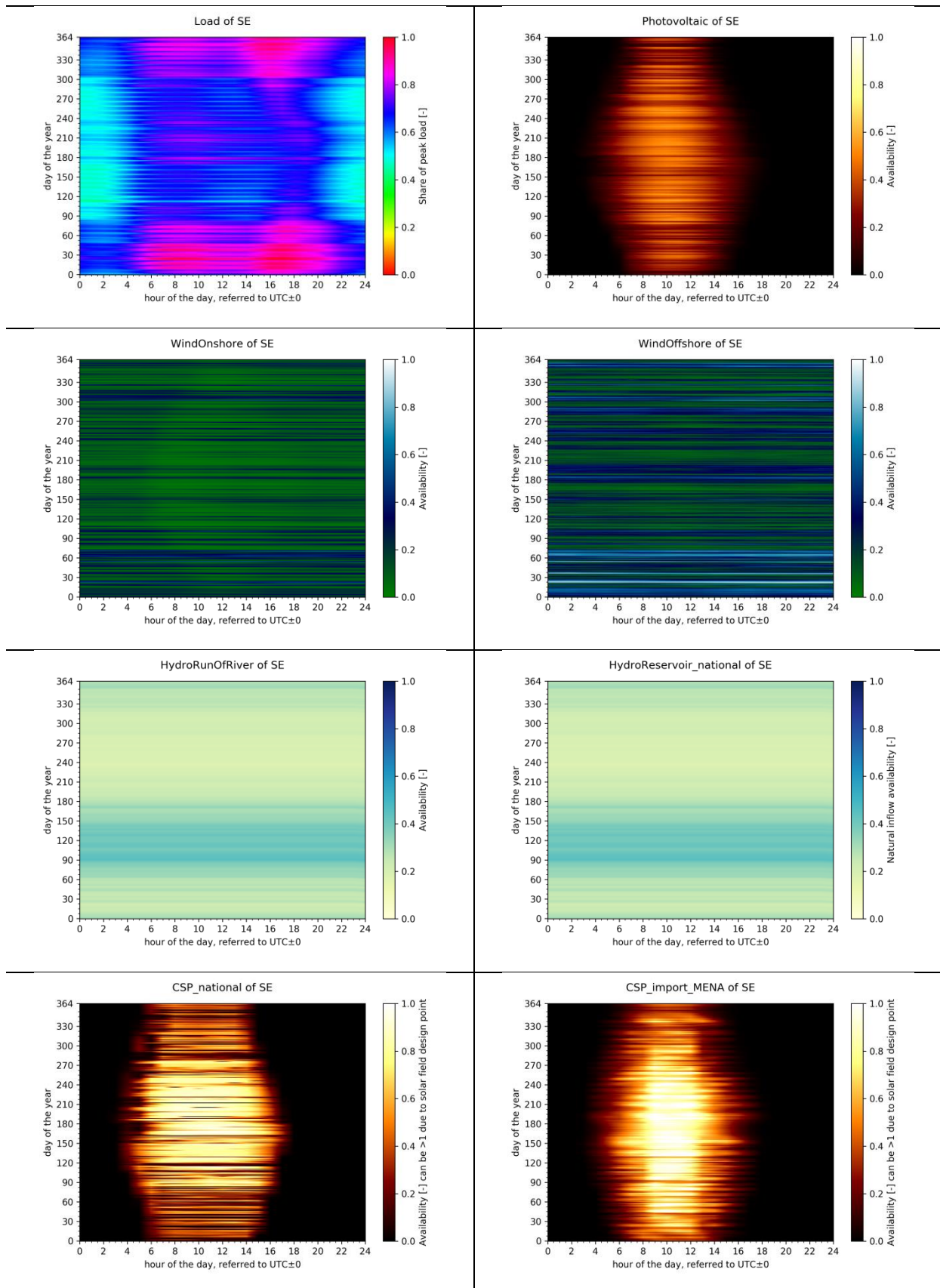
Figure 14: Load and technological time series of model region SE
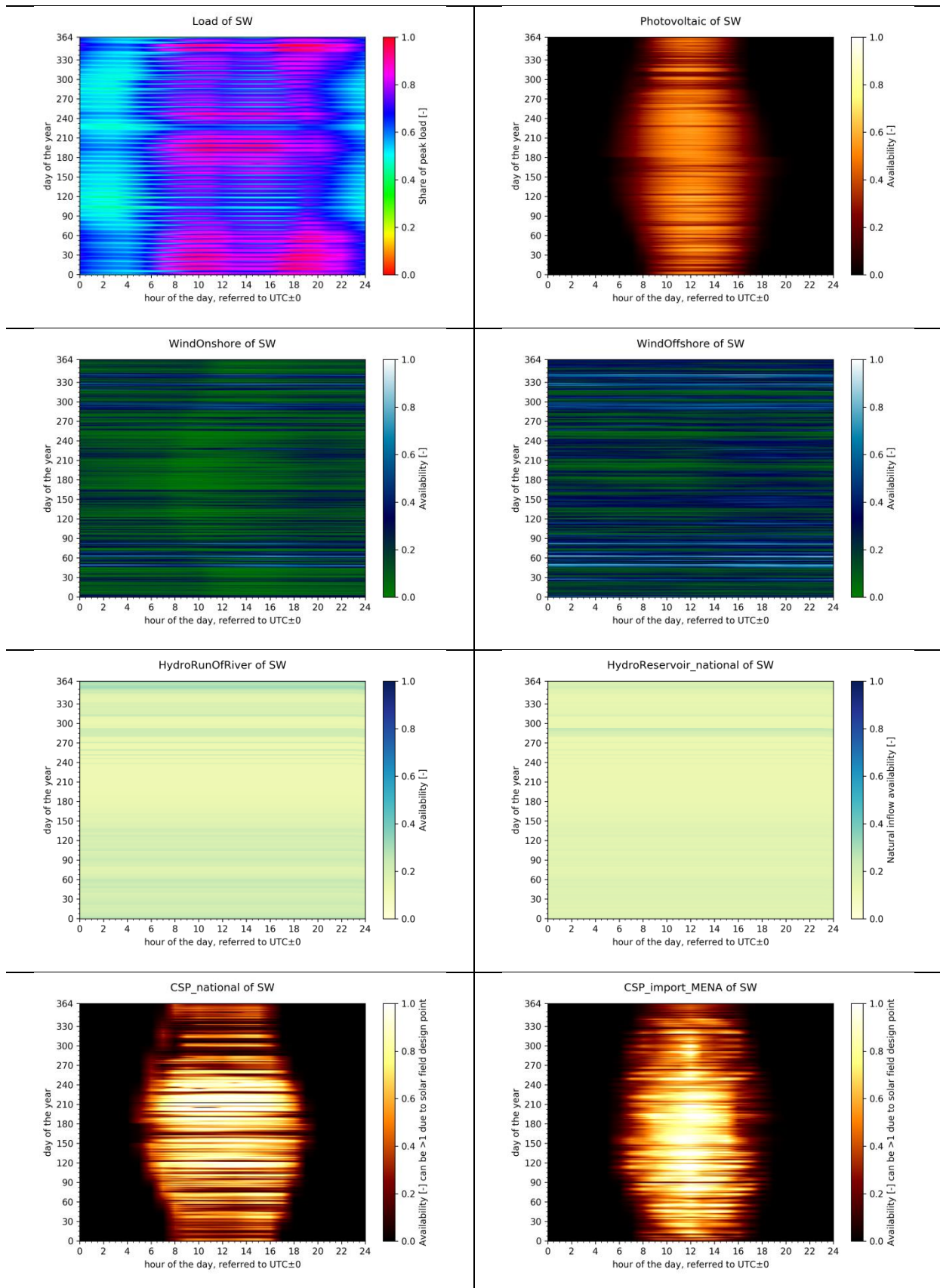
Figure 15: Load and technological time series of model region SW
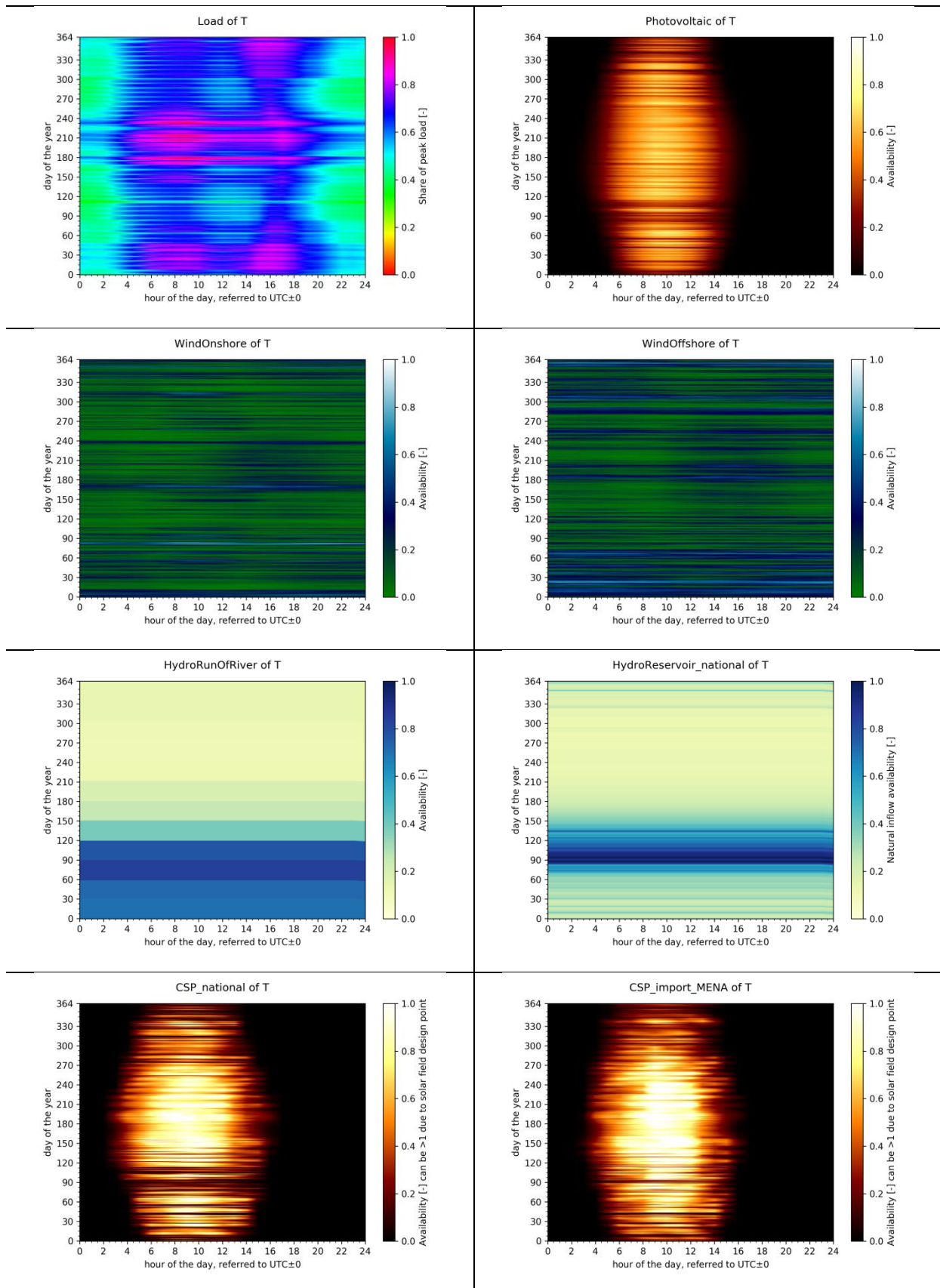
Figure 16: Load and technological time series of model region T
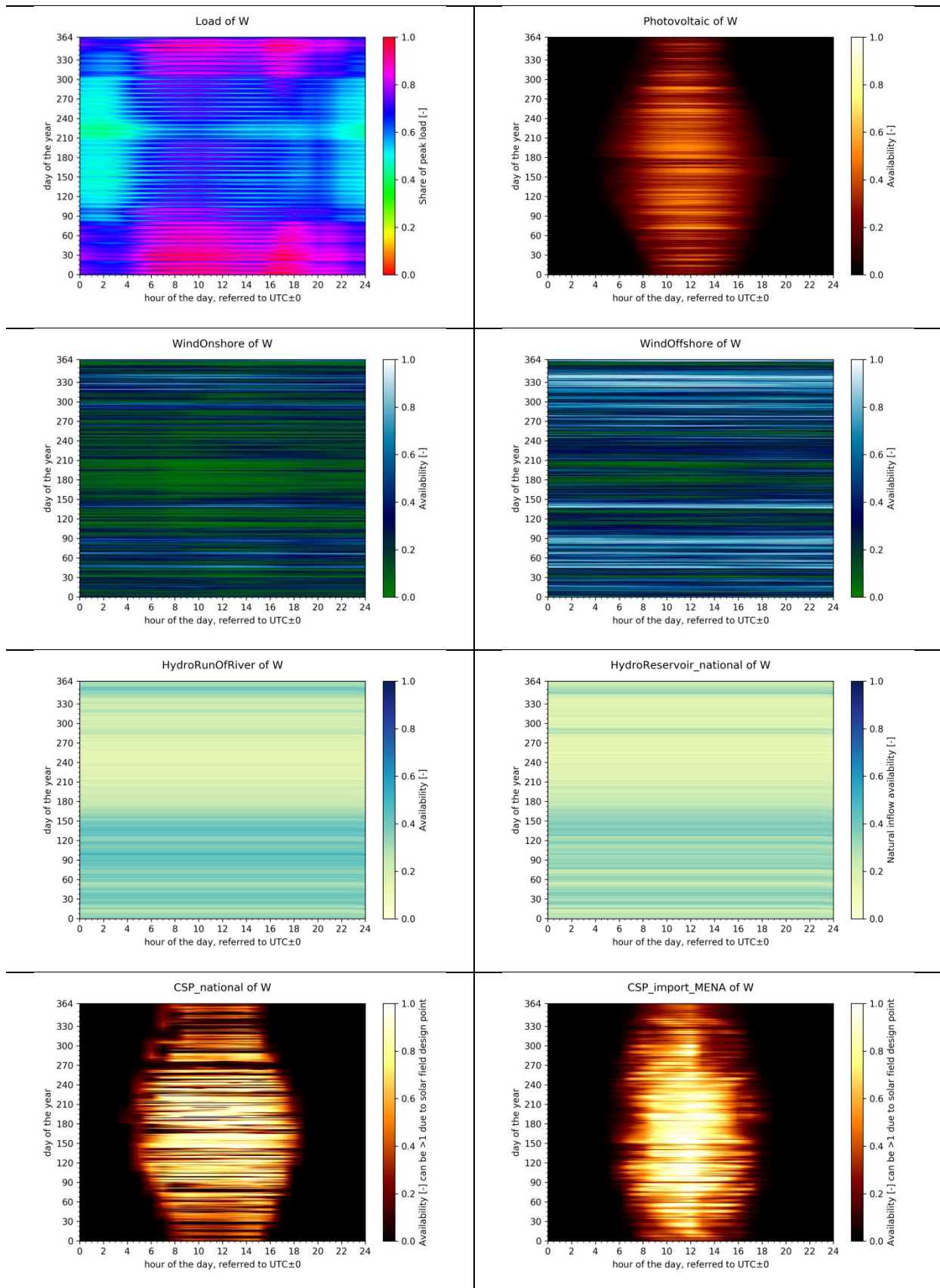
Figure 17: Load and technological time series of model region W

MENA:
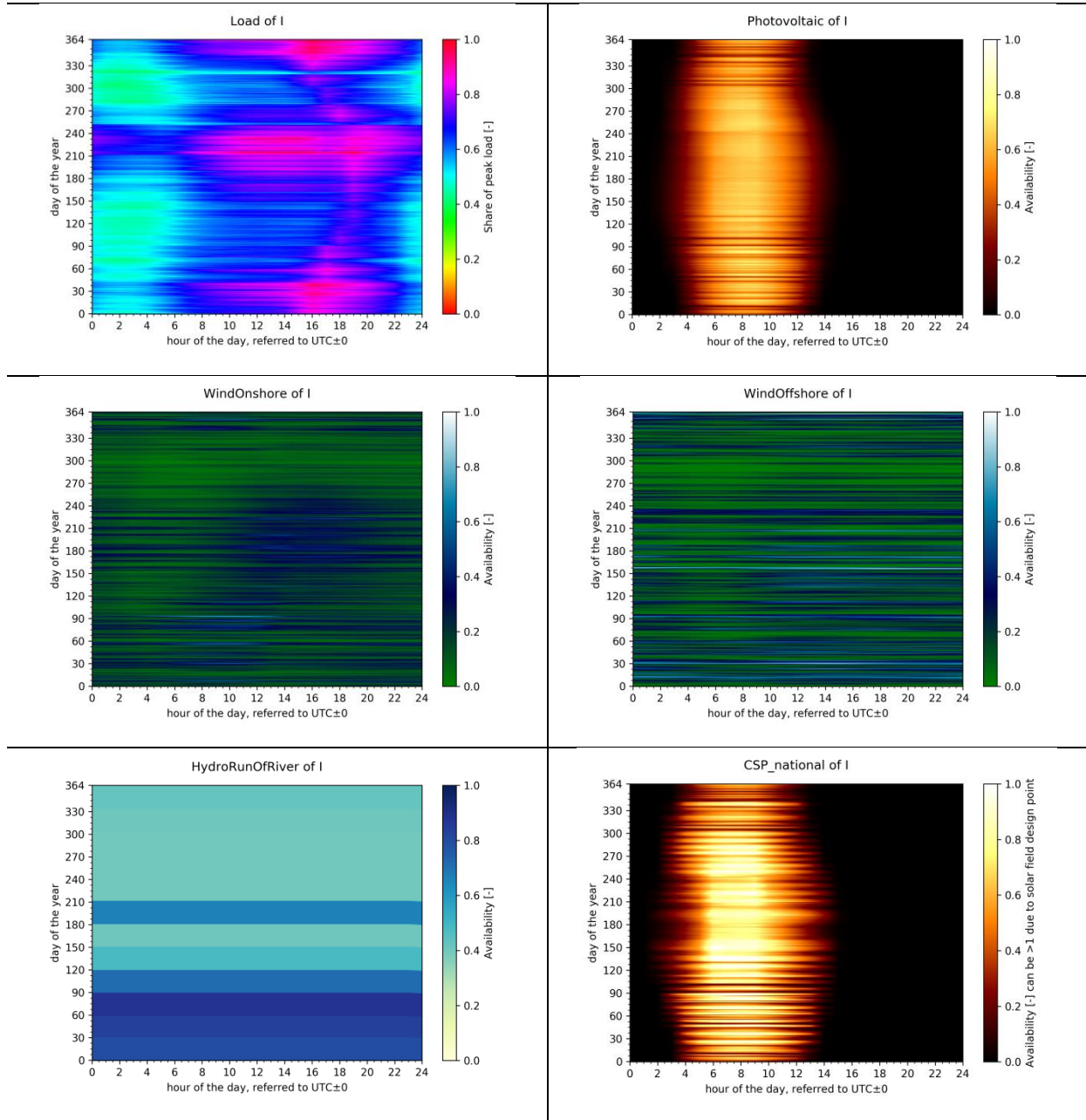
Figure 18: Load and technological time series of model region I
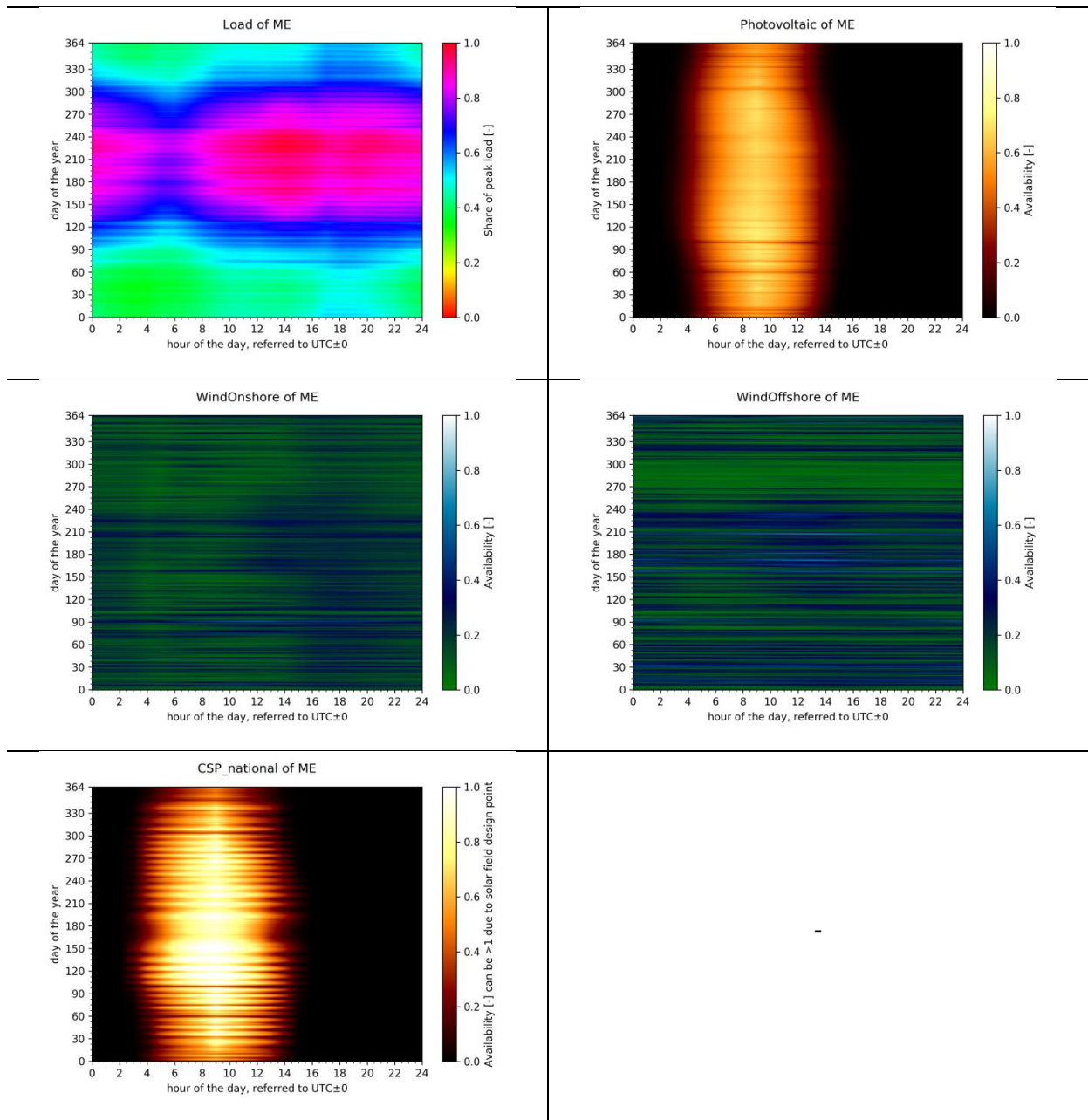
Figure 19: Load and technological time series of model region ME
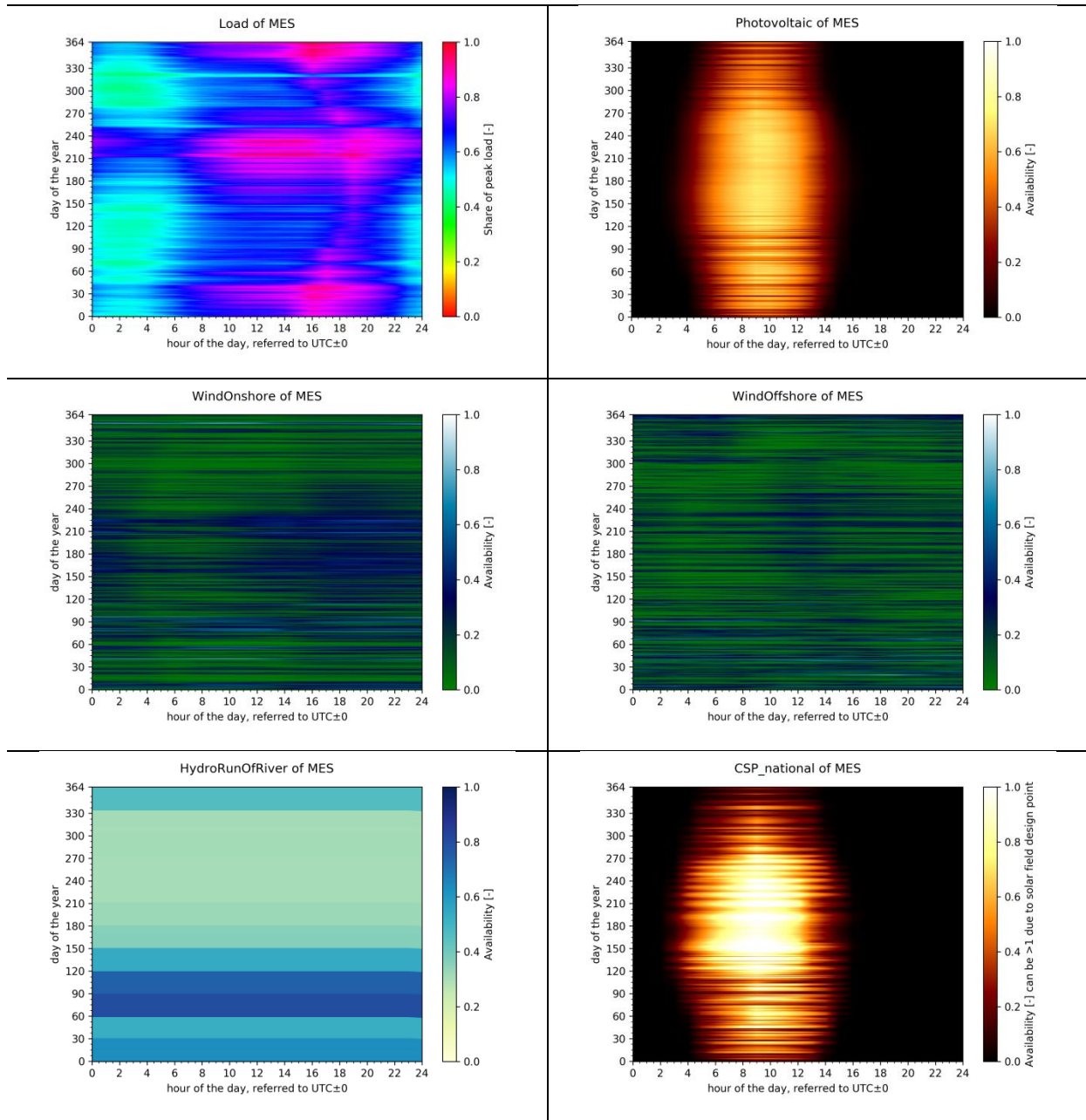
Figure 20: Load and technological time series of model region MES
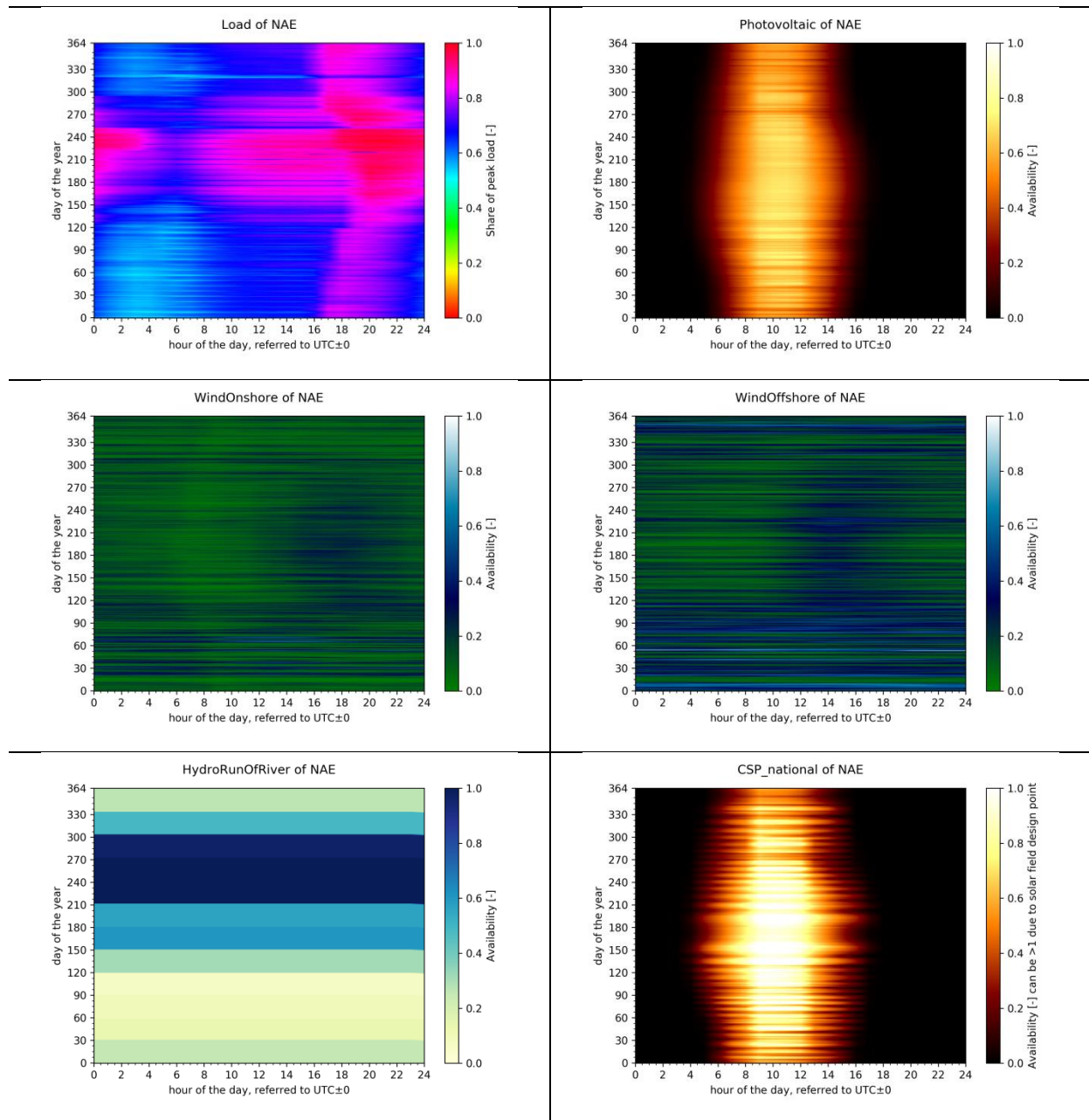
Figure 21: Load and technological time series of model region NAE
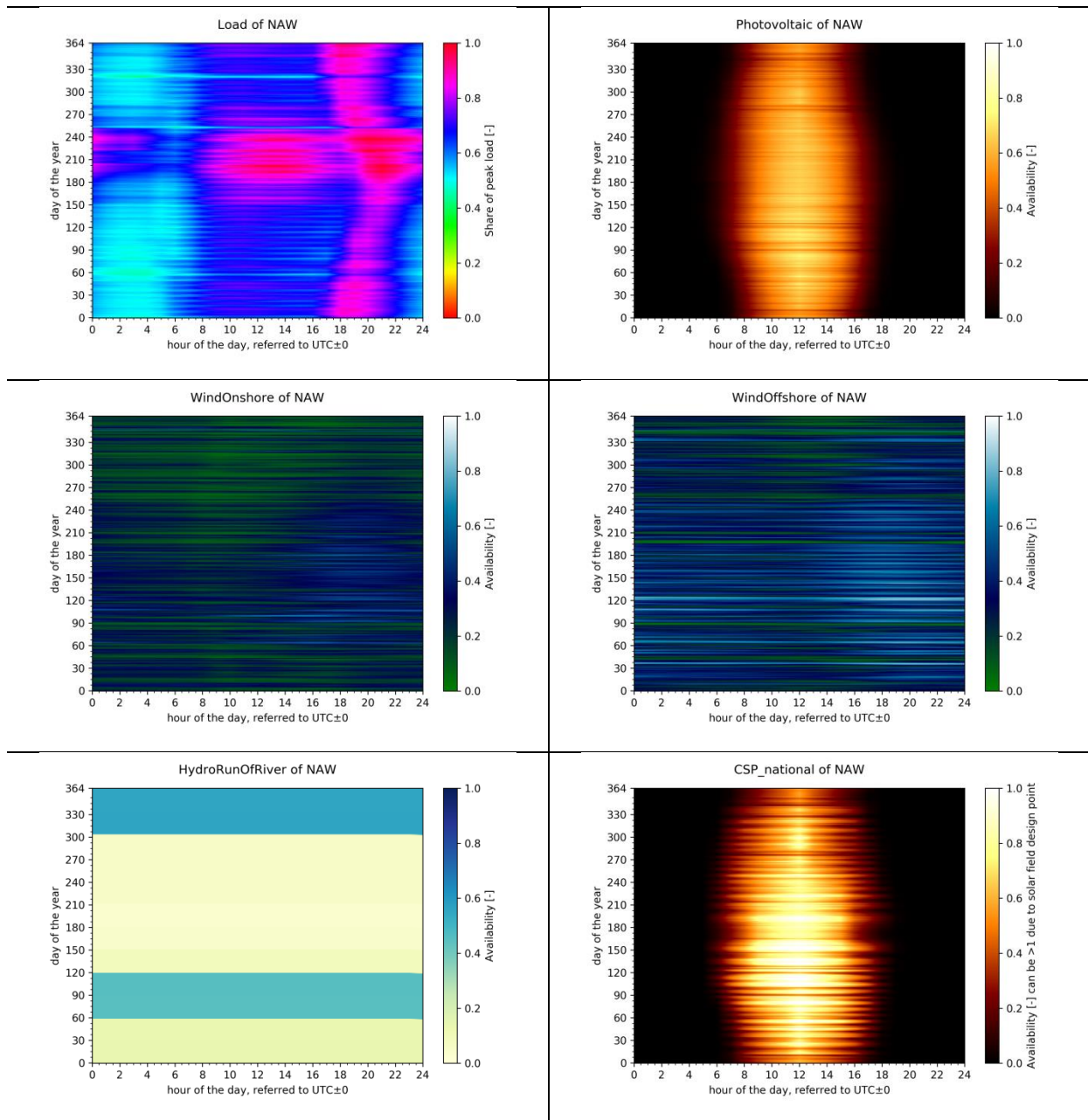
Figure 22: Load and technological time series of model region NAW

8.1.4 **Demand Side Management**

Regarding Demand Side Management (DSM), former studies have shown that the economic potential of DSM in Germany is approximately 10 GW [27] [28]. DSM substitutes short time storages (e.g. lithium ion batteries) and cost-efficient gas turbines [27] [28]. Thus, DSM has only a small influence on system cost and operating behaviour of the power plant park in Germany [27] [28]. Therefore DSM is neglected in the analysis.

8.1.5 **Storages**

The model uses different types of storage: short-term (e.g. battery type, represented by parameters for lithium ion batteries), medium-term (e.g. compressed air and pump storages) and long-term storages (e.g. hydrogen storages). The representatives are chosen due to the optimization method with the target function of minimizing system cost. When modelling technologies with about the same cost, the optimizer always uses the cheapest technology. Other technologies with about the same characteristics are therefore excluded by the optimizer. Thus, only the used three types of storage are considered due to their different temporal commitment.

Power-to-Gas-to-Power (P2G2P) is modelled with an electrolysis (alkali in maximum cost sensitivity, PEMFC in minimum cost sensitivity), methanation, compressed and stored in a salt cavern or in the gas distribution grid and burned in gas turbines. Power capacity of electrolyser and turbine can be optimized separately.

8.1.6 **Security of supply**

To ensure security of supply, the capacity credit is introduced (see Table 12). The capacity credit defines revision and outage of the installed capacity of each technology as an empirical value. For security and reserve reasons, the total firm capacity (product of capacity credits and related power plant capacities) must be 100%. So the total firm capacity is calculated referred to peak load at about 105%. To ensure firm national capacity in Germany, gas turbines are installed to cover the total peak demand together with other national dispatchable capacities in case of any failure. Installation of back-up capacities raise new financing questions if these capacities were not used (e.g. apportionment financing). CSP-HVDC is assumed with a capacity credit of 0% to model a possible total outage based on non-technical reasons. However, this dispatchable technology is able to ensure firm capacity due to its co-firing option. Thus, CSP-HVDC could substitute national gas turbines and reduce system cost if firm capacity abroad is accepted as such.

8.1.7 **Modelling of CSP-HVDC in REMix**

8.1.7.1 CSP-HVDC

A CSP-HVDC power plant is modelled with a solar field (SF), thermal energy storage (TES), power block (PB) with co-firing system (BUS), two HVDC converters and a HVDC transmission. Each of these components has its own techno-economic characteristics which

are listed in Table 12 and Table 17 and are considered by REMix. The following description is based on [13] and reveals the functioning of the CSP model with thermal storage and co-firing option in REMix.

The total solar field thermal capacity is composed of the exogenous capacity $Q_{existCap}$ and the model endogenous capacity $\boldsymbol{Q}_{addedCap}$ and is limited to the total potential calculated by REMix-EnDAT. The solar field thermal output $\boldsymbol{Q}_{SF}(t)$ arises from the overall capacity $(\boldsymbol{Q}_{addedCap} + Q_{existCap})$ and the normalised hourly availability of the solar resource $s_{gen}(t)$ as thermal time series. This is described in Eq. (10).

$$\boldsymbol{Q}_{SF}(t) \overset{!}{=} \left(\boldsymbol{Q}_{addedCap} + Q_{existCap}\right) \cdot s_{gen}(t) \qquad \forall t \qquad (10)$$

[13]

The thermal balance of CSP plants includes the thermal output of a solar field $\boldsymbol{Q}_{SF}(t)$, backup unit $\boldsymbol{Q}_{BUS}(t)$, TES charging $\boldsymbol{Q}_{charge}(t)$ and discharging $\boldsymbol{Q}_{discharge}(t)$, the thermal curtailment of the solar field $\boldsymbol{Q}_{curtail}(t)$, the power generation of the power block $\boldsymbol{P}_{gen}(t)$ according to Eq. (11) and the efficiency of the power block $\eta_{generator}$. The efficiency of the power block is the product of the thermal and electrical efficiency.

$$\boldsymbol{Q}_{SF}(t) + \boldsymbol{Q}_{BUS}(t) + \left(\boldsymbol{Q}_{discharge}(t) - \boldsymbol{Q}_{charge}(t)\right) - \boldsymbol{Q}_{curtail}(t) \overset{!}{=} \frac{\boldsymbol{P}_{gen}(t)}{\eta_{generator}} \qquad \forall t \qquad (11)$$

Hourly changes in TES energy level $\boldsymbol{U}_{level}(t)$ are described by the storage balance, which accounts for charging, discharging, and self-discharging in Eq.(12). An additional equation sets the storage level in the first and last time step to the same value, assuring that no energy is produced in the storage [13].

$$\boldsymbol{U}_{level}(t) \overset{!}{=} \boldsymbol{U}_{level}(t-1) + \left(\boldsymbol{Q}_{charge}(t) \cdot \eta_{charge} - \frac{\boldsymbol{Q}_{discharge}(t)}{\eta_{discharge}}\right) \cdot \Delta t - \frac{1}{2} \qquad (12)$$
$$\cdot \left(\boldsymbol{U}_{level}(t) + \boldsymbol{U}_{level}(t-1)\right) \cdot \eta_{self} \qquad \forall t$$

[13]

The hourly output of the power block $\boldsymbol{P}_{gen}(t)$ is limited by the available capacity. The storage level $\boldsymbol{U}_{level}(t)$ must be in all time steps lower than the overall TES capacity [13].

The novelty of modelling does not consist in the CSP model - developed by [11], [18] and [13] - but in the method of implementing CSP-HVDC in REMix. A CSP-HVDC power plant

transmits electricity via HVDC point-to-point transmission line directly to one offtaker in Europe. Thus, for this offtaker CSP is available apparently locally like home-grown renewable energies. Therefore CSP-HVDC is modelled as a power plant which has the solar resource of a MENA country and HVDC transmission losses - occurring with the transmission of CSP generated electricity to the consumer - but CSP from MENA is placed virtually in a European region. The gross capacity of the HVDC line $P_{HVDC,gross}$ is the same as the net capacity of the CSP power block $P_{PB,CSP,net}$ as described in Eq. (13).

$$P_{PB,CSP,net} = P_{HVDC,gross} \qquad (13)$$

Transmission losses are assumed to increase linearly with an increasing distance.

8.1.7.2 CSP sites, HVDC point-to-point transmission corridors and offtaker points

The basis for the CSP-HVDC power plant modelling is built by an exemplary identification of 15 CSP sites (hotspots) in MENA and 82 potential offtakers in geographical Europe (Figure 26 and Figure 27). These production and offtaker centres define the starting and end point of a CSP-HVDC power plant in the model. CSP hotspots are chosen selecting good solar resource [3], short distance to Europe and diversified placement in different MENA countries. The CSP resource is taken within a 30km radius of the hotspot. Offtakers are bigger EU cities that represent centres of demand.

The pathways of HVDC between these CSP hotspots and offtaker are calculated using a line laying algorithm [29]. This algorithm considers the geographical terrain with cost and minimizes cost to find a cost optimal pathway. Its spatial resolution is 1km x 1km.

The transmission pathway is calculated according to excluded areas (highest cost), preferred and unprivileged areas (lower or higher cost). Here two geographical categories are essential: The first category is independent from the direction of a pathway which is called isotropic friction image. The second category is dependant from the direction of the pathway and called anisotropic friction image (such as slope). With both categories cost-distance images of the CSP hotspots are calculated. Including the offtaker (demand centre) in the analysis a cost optimal pathway can be calculated with the cost-distance image.
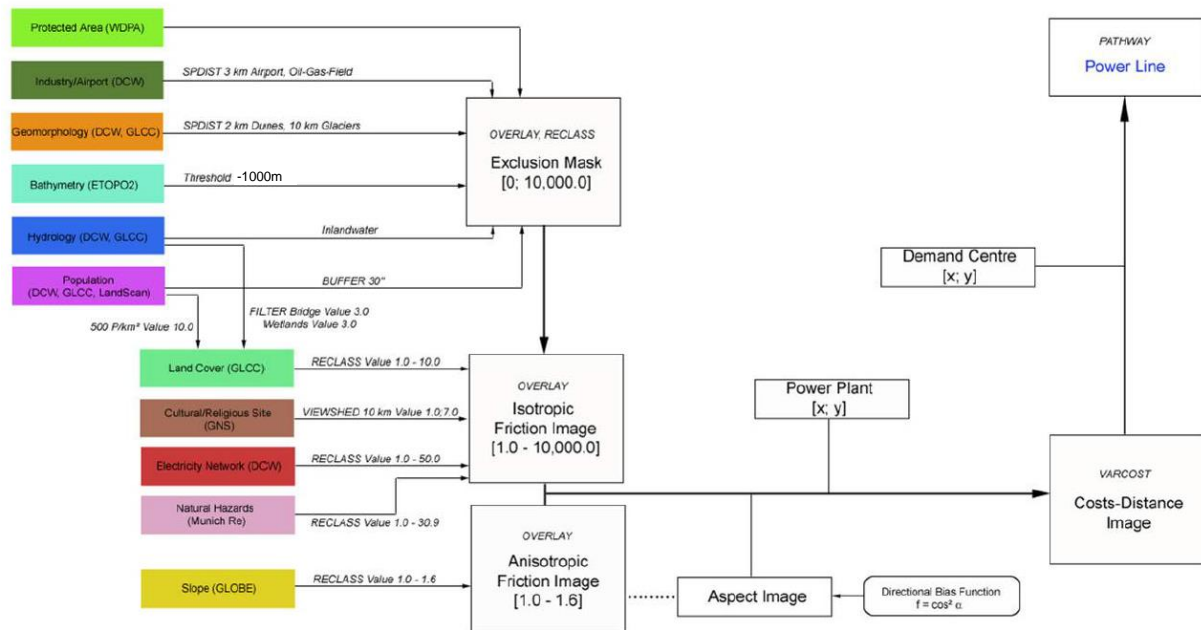
Figure 23: Line laying model based on [29]

The used isotropic friction images are exhibited in Figure 24 and Figure 25 showing two cost sensitivities:

- In Figure 24 a business as usual cost assumption is assumed which leads to predominant onshore pathways as shown in [29] and [3].
- In Figure 25 a dominant use of offshore pathways results. Here the isotropic friction image was calculated like in Figure 24 but with an addition of its highest sea cost value (~40) to the existing cost assumption of the land area.

Out of all possible combinations with 15 CSP sites and 82 potential offtakers (1230 possibilities) those CSP-HVDC plants are chosen which have a short distance to the consumer and at the same time a diversified solar resource from different CSP sites. Both figures illustrate the same connections between CSP hotspot and offtaker with different pathways. Evaluating CSP-HVDC in this paper with an energy system model presumes a reduction of this high-resolution infrastructure due to computational limits. Thus, average transmission lengths and average solar resource from selected CSP-HVDC are used each for one model region. The total average length to one model region is between 1200km and 3800km and is listed in Table 2. The average solar resource is shown by full load hours of the solar field in the appendix in Table 11. These solar resources of the CSP hotspots are assumed as relative conservative compared to the spatial average solar resources of a model region.

Figure 26 and Figure 27 illustrate a possible topology of CSP-HVDC. It is visible that in Figure 27 more straight pathways occur than in Figure 26 due to total higher cost. Thus, it can be assumed that Figure 27 represents sea cable and also underground cable. The CSP power plant sites and offtakters are exemplary and do neither represent real projects nor feasibility studies.
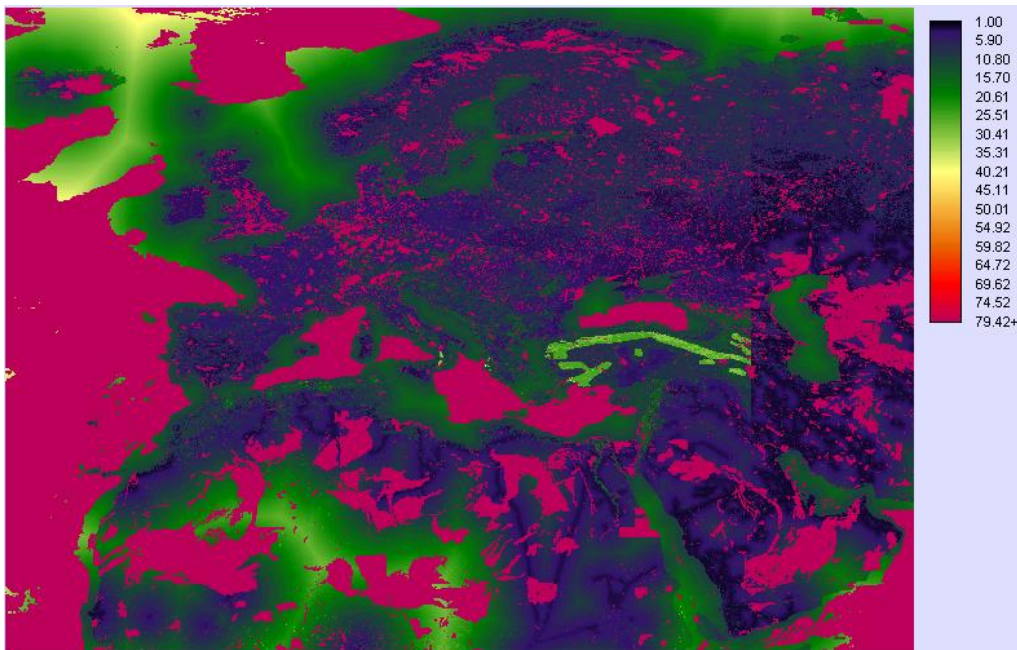
Figure 24: Isotropic friction image based on [29] (OHL case)
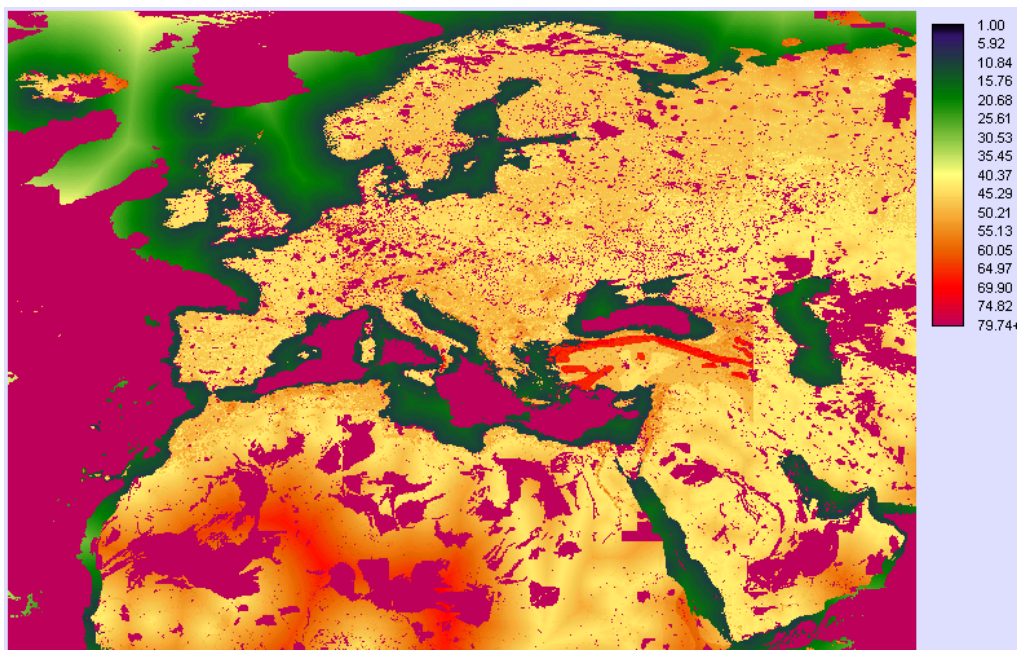
Figure 25: Isotropic friction image based on [29] with addition of highest sea cost value (~40) to all land cost values allowing the algorithm to use predominantly offshore pathways (sea cable and UGC case)
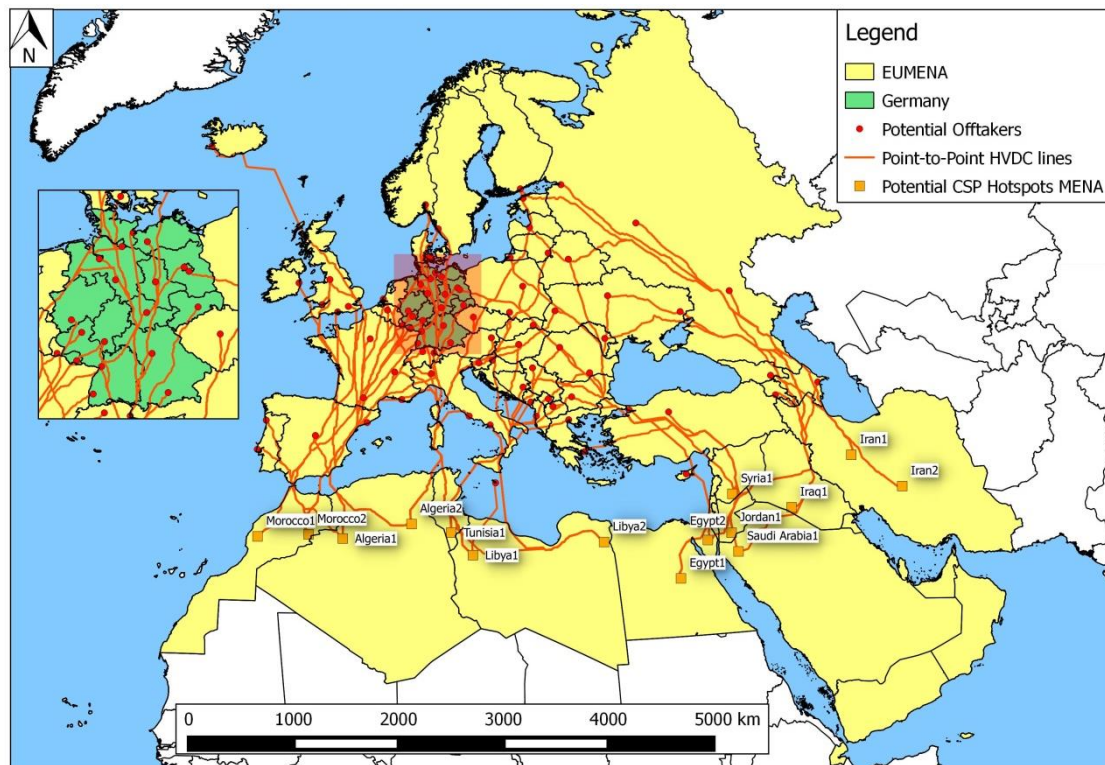
Figure 26: Point-to-point CSP-HVDC with potential CSP hotspots in MENA and potential offtakers in Europe – predominant onshore line configuration (OHL case)
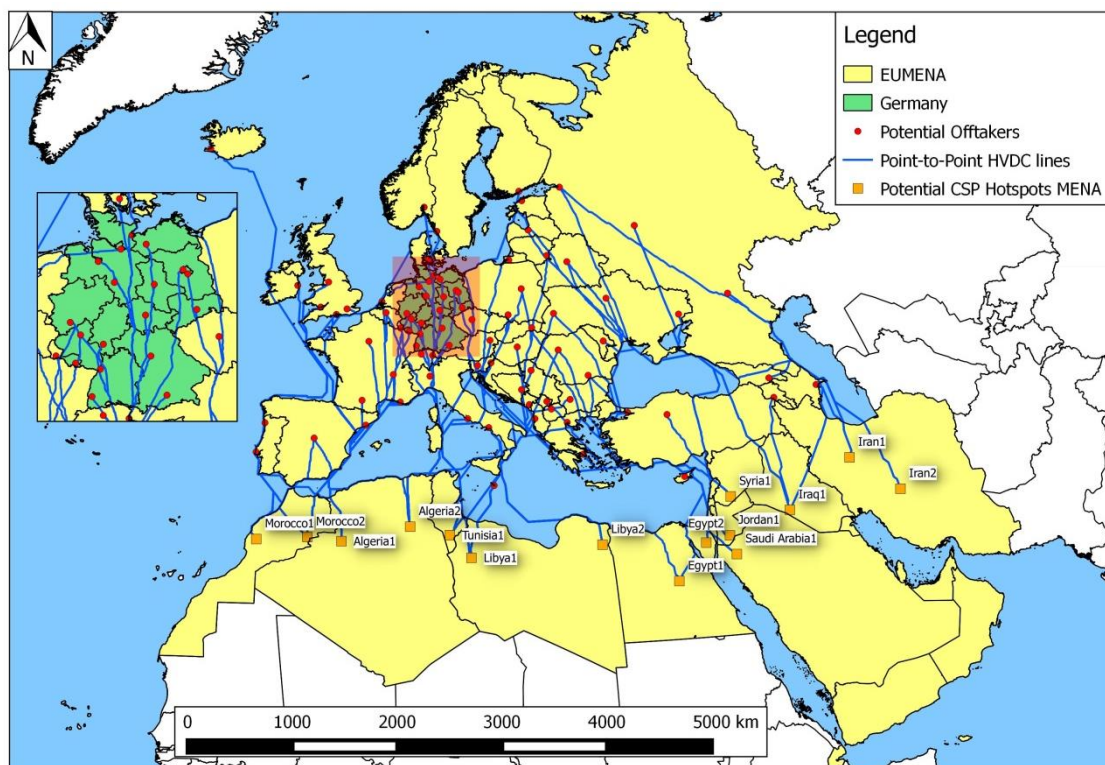
Figure 27: Point-to-point CSP-HVDC with potential CSP hotspots in MENA and potential offtakers in Europe – predominant offshore configuration (sea cable and UGC case)

For Germany a relatively high number of offtakers is included to identify precisely the average length of a specific point-to-point line.

8.1.8 Supply technologies and their resource potentials

Table 10 shows the model limitations by resource potential of the listed technologies. Other used technologies or technological components (e.g. storage size) have unlimited potentials.

Table 10: Limited resource potentials of used technologies

Technology/ Model region	Pump storage discharge [MW$_{el}$]	Hydro run-of-river [MW$_{el}$]	Hydro-reservoir regional, turbine [MW$_{el}$]	Hydro-reservoir import from N, turbine [MW$_{el}$]*	Geothermal energy [TWh$_{el}$]	Solid biomass [TWh$_{chem}$]	CSP regional, solar field [GW$_{th}$]
G	15875	4377	430	6153	26	216	0
N	4781	39326	25813	-	1	832	0
E	3500	4504	963	3748	17	338	0
S	20014	31924	16500	-	18	317	105
W	7743	13943	11660	-	12	329	19
NW	3853	3507	328	7308	24	57	0
NE	2612	32448	0	-	1	2580	0
SE	4149	21721	8330	-	8	520	42
NAE	0	3033	0	-	13	12	242239
NAW	932	1724	0	-	9	80	234089
SW	19588	8560	12999	-	22	314	1566
T	571	14611	679	-	75	212	373
MES	0	3313	0	-	0	12	58426
I	0	1044	0	-	6	38	37867
ME	0	0	0	-	68	3	224692

*The import potential of hydro reservoir from model region N to G, E and NW is calculated with 40% of the available potential in N and distributed due to the electricity of the destination model regions. Thus, 60% of the original potential remains in model region N.

Potential of pump storage discharge is taken from [30] "T2 realisable (5km)" with energy to power ratio of 7 and a reduced potential of 75.5%. This reduced potential is achieved comparing the cost-efficient pump storage discharge potential in Germany of 15GW [31] to the study values with 20GW [30]. Potential of hydro run-of-river and CSP is taken from [11]

for Europe and from [12] for MENA. Potential of hydro-reservoir is taken from [32] using a power plant matching in Europe and for Turkey from [11]. Potential of geothermal energy is taken from [1], [2] and for Germany from [33]. Net primary production (NPP) potential of solid biomass is taken from model values of [34]. The assumed usable energy potential consists of 25% of total tree NPP and of 20% of total straw NPP of the year 2010.

8.1.9 Annual characteristic of load and renewable resources

For a regional comparison of renewable resources and demand Table 11 shows peak load and average full load hours of model regions.

Table 11: Peak load and average resource full load hours of model regions

Model region	Peak Load [GW]	Average resource full load hours [h/y]					
		PV	Wind Onshore	Wind Offshore	Hydro Run Of River	CSP solar field national	CSP solar field import
G	112	836	2107	4125	5015	-	1934
N	99	867	2023	3810	4137	-	1980
E	69	1016	1731	3207	2396	-	2011
S	112	1139	1353	1917	3033	1914	1943
W	155	1027	2110	3626	2543	1881	1926
NW	134	789	3721	4309	3606	-	1916
NE	170	1011	2251	3260	3220	-	1939
SE	54	1118	1290	2265	2432	1938	1997
NAE	182	1747	1257	1939	4219	2135	-
NAW	112	1701	2179	3096	1925	2026	-
SW	57	1309	1555	2418	1551	2034	1897
T	113	1494	1312	1767	3266	1847	1966
MES	165	1620	1661	1400	4096	1881	-
I	152	1671	1591	1725	4957	1972	-
ME	170	1749	1577	1765	-	2105	-

The average resource full load hours are a result of an aggregation of the spatial availability of the resource. Full load hours of CSP solar field import represent an average of selected

sites in EUMENA which leads to a more conservative approach than for CSP solar field national.

8.2   Used techno-economic data

The objective of the analysis is to model CSP-HVDC and CSP relative conservatively compared to other technologies. This facilitates a conservative examination of CSP-HVDC and CSP to analyse their value strictly avoiding an overestimation of this technology. Therefore the applied techno-economic data for other technologies are rather optimistic.

The bandwidth of cost assumptions ($€_{2015}$) and technological characteristics in Table 12 to Table 18 are assumed from today's point of view and can differ from reality especially when projecting an energy system in the year 2050.

Table 12 to Table 18 include an exchange rate with 1$ at the parity of 1.35 €. Some values are based on a time value of money the year 2010. Therefore an inflation rate of 10% is considered from 2010 to 2015 to calculate the time value of money of the year 2015. The mean values are not listed in the tables but are calculated according to the average of max and min values.

Table 12: Cost and technology parameters for power plants in the year 2050 based on expert assumptions

Technology	Cost sensitivity	Specific investment [k€/MWel]	O&M Fix [%/y] of investment	O&M Variable [€/MWh]	Fuel cost [€/MWh]	Amortisation Time [y]	Interest Rate	Efficiency [-] net	Availability	Capacity Credit [-]
Photovoltaics	max	1150	0.04	0.00		20	9%	1	98%	0
	min	597	1.10	0.00		40	3%			
Wind Onshore	max	1272	2.10	4.33		18	9%	1	95%	0
	min	769	1.61	2.44		24	3%			
Wind Offshore	max	2275	3.64	13.87		16	9%	1	95%	0
	min	1052	3.49	9.55		22	3%			
Run-Of-River	max	5541	5.50	4.84		40	9%	1	95%	0
	min	5541	2.75	2.44		60	3%			
Hydro Reservoir*	max	2113	5.00	1.00		40	9%	1	98%	0
	min	1017	5.00	1.00		30	3%			
Solid Biomass	max	3833	1.98	3.20	40.0	20	9%	0.35	90%	0.9
	min	1647	5.60	2.90	25.0	30	3%			
Geothermal	max	6797	3.00	0.10		20	9%	1	90%	0.9
	min	3826	3.00	0.10		30	3%			
CSP power block	max	1098	2.50	2.22		35	9%	0.37	95%	modelled with 0, however 0.9 is possible accepting firm capacity abroad
	min	857	2.50	2.22		45	3%			
CSP solar field	max	356 k€/MW$_{thermal}$	2.50			20	9%		95%	-
	min	166 k€/MW$_{thermal}$	2.50			30	3%			
CSP thermal storage	max	18 k€/MWh	2.50			20	9%	0.95 and 0.05%/h self-discharge rate	95%	-
	min	11 k€/MWh	2.50			30	3%			

Sources: [35], [36], [37], [38], [39], [40], own assumptions

Table 13: Cost and technology parameters for storages in the year 2050

Technology	Cost sensitivity	Specific investment [k€/MWel]	O&M Fix [%/y] of investment	O&M Variable [€/MWh]	Amortisation Time [y]	Interest Rate	Efficiency [-] net	Availability	Capacity Credit [-]
Pump Storage storage	max	40 k€/MWh	2.80	-	30	9%	0%/h self-discharge rate		-
	min	5 k€/MWh	1.86	-	40	3%			
Pump Storage charge	max	400	2.80	3.80	20	9%	0.89	95%	-
	min	180	1.86	3.80	30	3%			
Pump Storage discharge	max	400	2.80	-	20	9%	0.90		0
	min	170	1.86	-	30	3%			
Power-to-Gas-to-Power (P2G2P) Storage	max	0.20 k€/MWh	3.00	-	25	9%	0%/h self-discharge rate		-
	min	0.20 k€/MWh	2.42	-	35	3%			
Power-to-Gas-to-Power (P2G2P) charge	max	1206 = 606 (alkali electrolysis) +600 (methanation)	3.00	2.30	15	9%	0.70 = 0.79 (methanation) x 0.89 (compression)	95%	-
	min	922 = 322 (PEM electrolysis) +600 (methanation)	2.42	1.64	20	3%			
Power-to-Gas-to-Power (P2G2P) discharge (gas turbine)	max	713	3.00	-	25	9%	0.465		0.95
	min	417	2.42	-	40	3%			
Compressed Air Storage storage	max	60 k€/MWh	1.30	-	25	9%	0.125%/h self-discharge rate		-
	min	38 k€/MWh	1.30	-	35	3%			
Compressed Air Storage charge	max	310	1.30	2.70	20	9%	0.88	95%	-
	min	200	1.30	0.10	30	3%			
Compressed Air Storage discharge	max	400	1.30	-	25	9%	0.70		0
	min	260	1.30	-	35	3%			
Lithium Ion storage	max	220 k€/MWh	2.00	-	15	9%	0.001%/h self-discharge rate		-
	min	150 k€/MWh	2.00	-	25	3%			
Lithium Ion charge	max	25	2.00	0.22	15	9%	0.97	95%	-
	min	12.5	2.00	0.22	25	3%			
Lithium Ion discharge	max	25	2.00	-	15	9%	0.97		0
	min	12.5	2.00	-	25	3%			

Sources: [41], [42], [43], own assumptions

Table 14: Cost and technology parameters for carbon emitting and nuclear technologies in the year 2050

Technology	Cost sensitivity	Specific investment [k€/MWel]	O&M Fix [%/y] of investment	O&M Variable [€/MWh]	Fuel cost [€/MWh$_{chem}$]	Amortisation Time [y]	Interest Rate	Efficiency [-] net	CO$_2$ sequestration [-]	Availability	Capacity Credit [-]
Coal CCS Steam Turbine	max	2460	4	9.2	30	25	9%	0.299	0.85	0.896	0.9
	min	1807	4	9.2	18.9	40	3%				
Coal Steam Turbine	max	1418	4	0.1	30	25	9%	0.509	0	0.896	0.9
	min	1108	4	0.1	18.9	40	3%				
Combined CCS Cycle Gas Turbine	max	1203	4	3.5	65.2	25	9%	0.428	0.86	0.96	0.9
	min	867	4	3.5	40.1	40	3%				
Combined Cycle Gas Turbine	max	691	4	0.3	65.2	25	9%	0.621	0	0.96	0.9
	min	491	4	0.3	40.1	40	3%				
Gas Turbine	max	713	4	0.3	65.2	25	9%	0.465	0	0.95	0.9
	min	417	4	0.3	40.1	40	3%				
Lignite Steam Turbine	max	1750	4	0.1	11.1	25	9%	0.491	0	0.902	0.9
	min	1250	4	0.1	9.1	40	3%				
Nuclear Steam Turbine	max	13030	4	0.1	5.5	25	9%	0.309	-	0.90	0.9
	min	4684	4	0.1	5	40	3%				

Sources: [40], [44], [45], [46], own assumptions, CCS O&M Variable are based on cost for CO$_2$ transport (3€/t) and CO2 storage (4.45 €/t) [47]

Table 15: Specific CO_2 emission

Fuel	tCO_2/MWh_{chem}
Coal	0.3348
Lignite	0.3996
Natural Gas	0.2016
Nuclear	0
Biomass	0

Source: [40]

Table 16: CO_2 certificate cost representing environmental impact

Cost sensitivity	$€/tCO_2$
max	82.5
mean	62.7
min	49.5

Source: [40]

Table 17: Techno-economic parameters of HVDC infrastructure

	DC	DC converter	Losses
OHL	786.000 €/km	148.730.000 € per station	4.5 %/1000km
UGC	2.271.350 €/km	148.730.000 € per station	3.5 %/1000km
Sea cable	2.672.000 €/km	148.730.000 € per station	2.7 %/1000km
Specific Capacity	1500 MW	1500 MW	
Specific Voltage	600 kV		

Losses of converter station are assumed with 0.7%. Sources: [48], [3], [49].

Table 18: Learning curve approach of CSP solar field, thermal storage and power block based on installed capacity and progress ratio

Cost sensitivity	Unit	Current state	MAX	MEAN	MIN	Unit	Progress Ratio MAX	Progress Ratio MIN
year		2015	2050	2050	2050			
Installed capacity	MW	4,700	120,000	835,000	1,550,000			
Solar Field	[k€/MWh$_{th}$]	647	355	260	166	[-]	0.88	0.85
Thermal Storage	[k€/MWh$_{th}$]	50	19	15	11	[-]	0.80	0.83
Power Block	[k€/MW$_{el}$]	1206	1098	978	857	[-]	0.98	0.96

Sources: based on [50] and [3], [51], [52], [53]

8.2.1 Node-internal transmission and distribution grid

In a novel approach the region internal grid is modelled respecting the main grid expansion drivers: wind and photovoltaics feed-in power into the grid. Grid expansion related to a rising demand is considered independently. The model is capable of making conclusions of grid expansion and curtailment of PV and wind energy in an optimized energy system. The region internal grid model is explained in [14]. The model uses two parameters to quantify the grid: start point of grid expansion in relation to peak load and specific cost per feed-in power of photovoltaics and wind turbines. The used parameters for each model region, distribution and transmission grid are listed in Table 19.

Table 19: Used parameters for distribution and transmission grid inside a model region

Grid	Distribution grid						Transmission grid				
	Start of grid expansion [% of peak load]			cost per fluc feed-in [€/kW]			Start of grid expansion [% of peak load]			cost per fluc feed-in [€/kW] (OHL)	cost per fluc feed-in [€/kW] (UGC)
Cost scenario	max	mean	min	max	mean	min	max	mean	min	max/ mean/min	max/ mean/min
G	53.5	60.5	73.4	409	375	500	20	25	30	584	899
N	53.5	60.5	73.4	409	375	500	20	25	30	801	1233
E	53.5	60.5	73.4	409	375	500	20	25	30	824	1269
S	53.5	60.5	73.4	409	375	500	20	25	30	647	997
W	53.5	60.5	73.4	409	375	500	20	25	30	582	896
NW	53.5	60.5	73.4	409	375	500	20	25	30	481	741
NE	53.5	60.5	73.4	409	375	500	20	25	30	1149	1769
SE	53.5	60.5	73.4	409	375	500	20	25	30	1253	1929
NAE	53.5	60.5	73.4	409	375	500	20	25	30	1331	2049
NAW	53.5	60.5	73.4	409	375	500	20	25	30	1939	2985
SW	53.5	60.5	73.4	409	375	500	20	25	30	1294	1991
T	53.5	60.5	73.4	409	375	500	20	25	30	1159	1783
MES	53.5	60.5	73.4	409	375	500	20	25	30	1288	1982
I	53.5	60.5	73.4	409	375	500	20	25	30	1227	1889
ME	53.5	60.5	73.4	409	375	500	20	25	30	517	795

8.3 Configuration of CSP-HVDC and CSP as a result of the empirical probability analysis

As additional results of the CSP-HVDC and CSP cost bandwidths, the technological configuration bandwidths are shown in Figure 28 by the solar multiple, in Figure 32 by the solar field capacity, in Figure 29 by the thermal energy storage, in Figure 30 by the electrical net generation and in Figure 31 by the electricity generation by co-firing. These results depend on the used cost sensitivities and show the difference between scenarios with 0 (first row of the figures – a,b) and 16 g CO_2/kWh_{demand} (second row of the figures – b,c) neglecting and including CCS (third row of the figures – e,f). The results show that high CO_2 emission and the inclusion of CCS leads to lower CSP configuration values.

The results of sensitivity analysis show in Figure 28 the bandwidths of the solar multiple in the analysed regions with boxplots. In the left column the CSP-HVDC technology and in the right column the CSP technology is described.
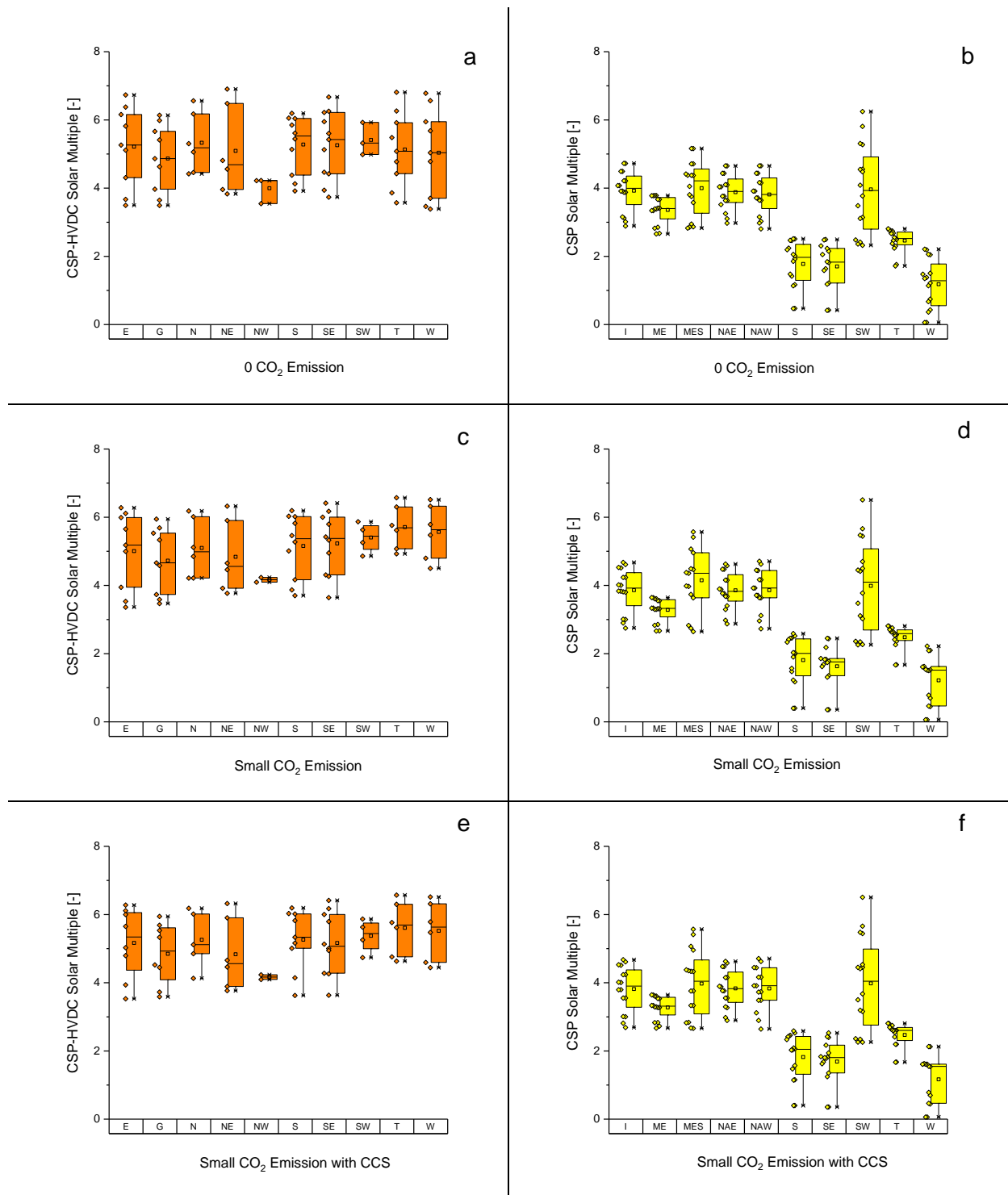
Figure 28: Solar Multiple
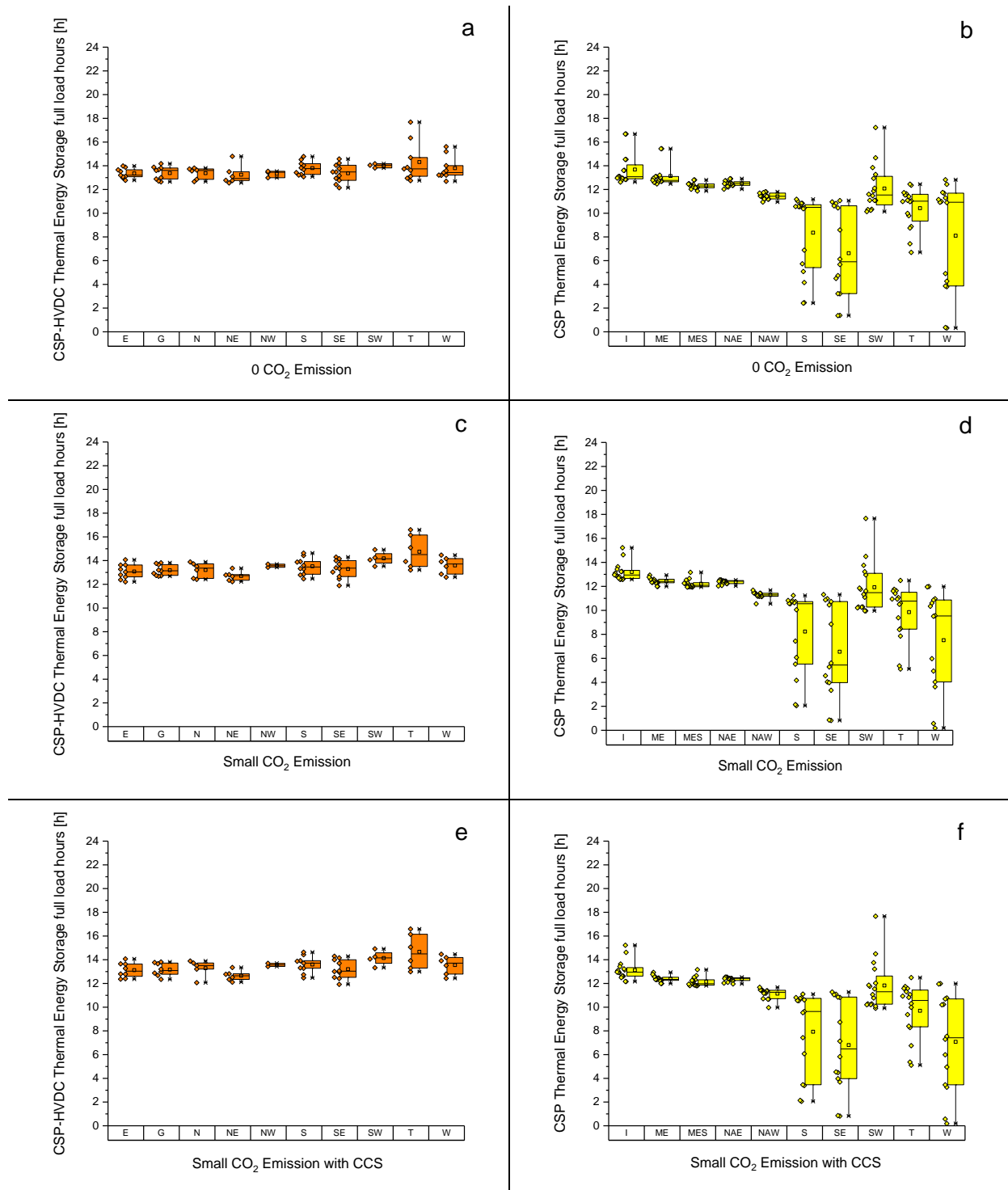
Figure 29: Thermal energy storage full load hours

Figure 30 shows the net electricity generation [TWh_{el}] from CSP-HVDC and CSP. In the MENA region (regions I, ME, MES, NAE and NAW) the net electricity generation is relative high due to a high share of CSP. Also the use of the thermal energy storage in Figure 29 is high compared to other regions in MENA.
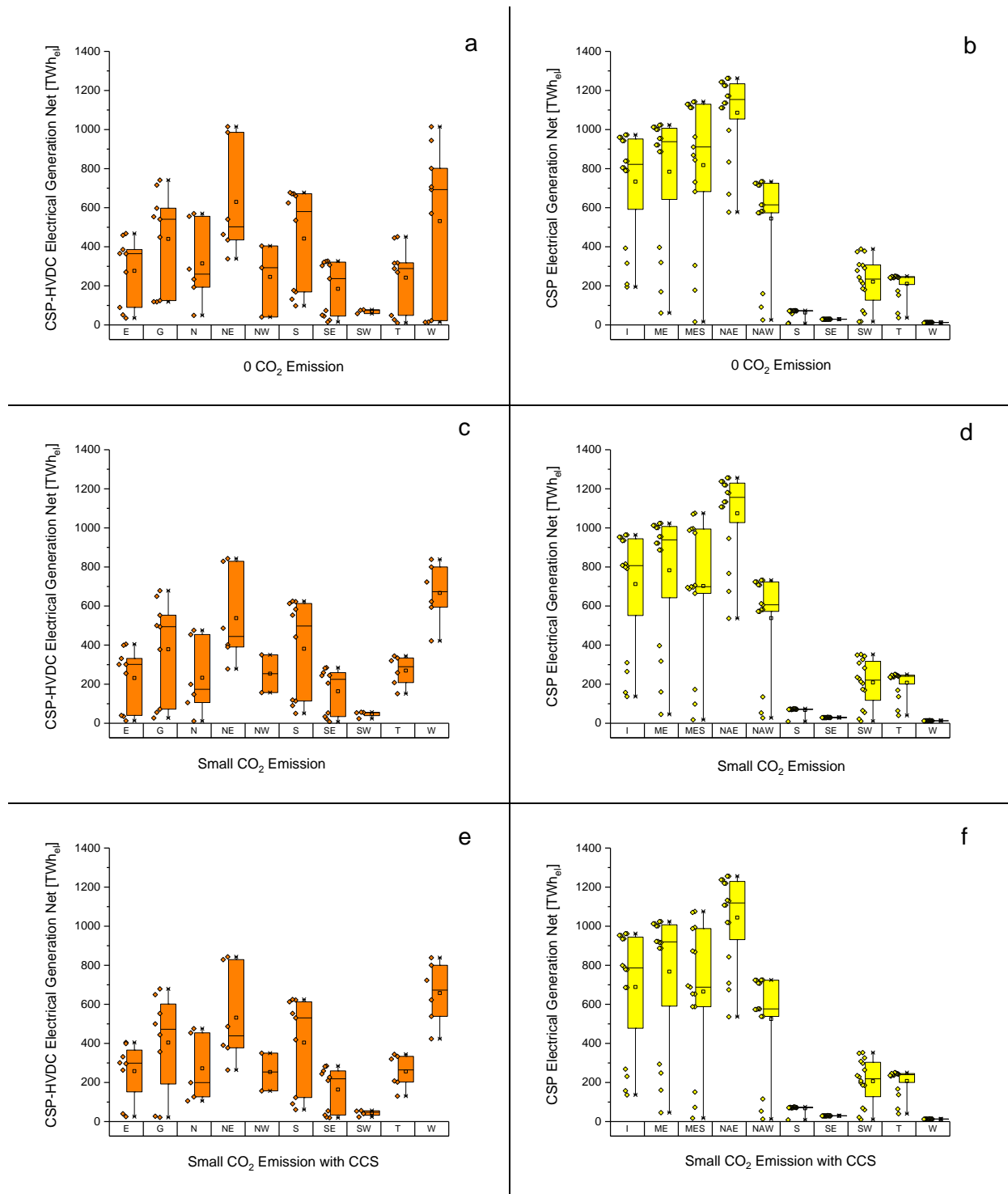

Figure 30: Electrical generation net of the CSP plant without transmission losses.

Figure 31 shows the co-firing with natural gas of the CSP-HVDC and CSP technologies. It can be seen in Figure 31d and f that the electricity generation using co-firing compared to the net electrical generation is low (comparison of Figure 31 and Figure 30). However, some regions have a higher absolute co-firing value. This is not a result of different demand but a consequence of an hourly misfit of renewable energies and the demand curve. The integration of CCS technologies (here CSP has no CCS possibility) leads to a higher co-firing. Thus, it is more efficient to use the co-firing of CSP when CCS is integrated.

| a	b
No co-firing with the use of natural gas in the scenario 0 CO_2 emission per definition	No co-firing with the use of natural gas in the scenario 0 CO_2 emission per definition
c	d
Model does not use co-firing for CSP-HVDC	
e	f
Model does not use co-firing for CSP-HVDC	
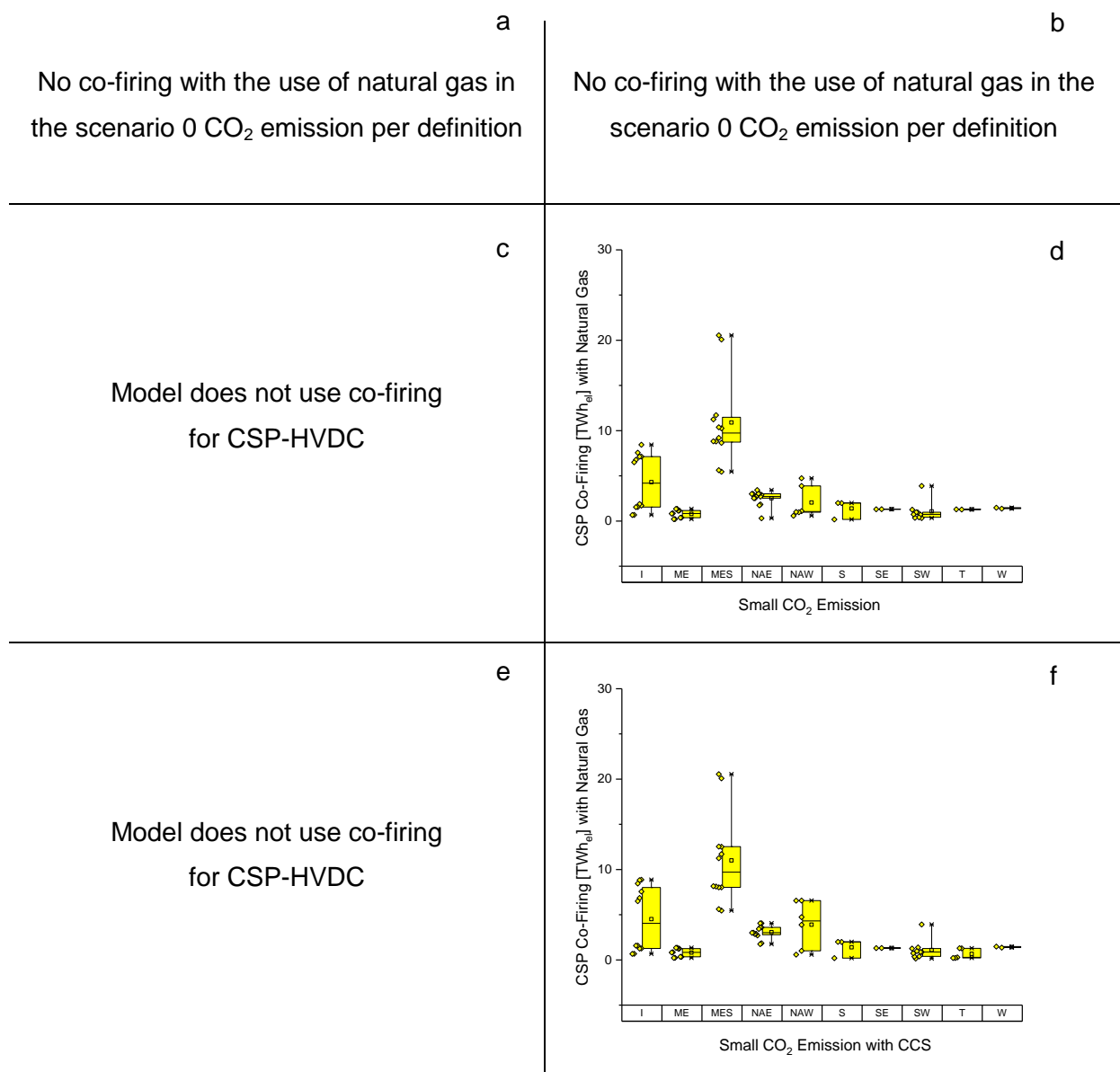
Figure 31: Co-firing with natural gas
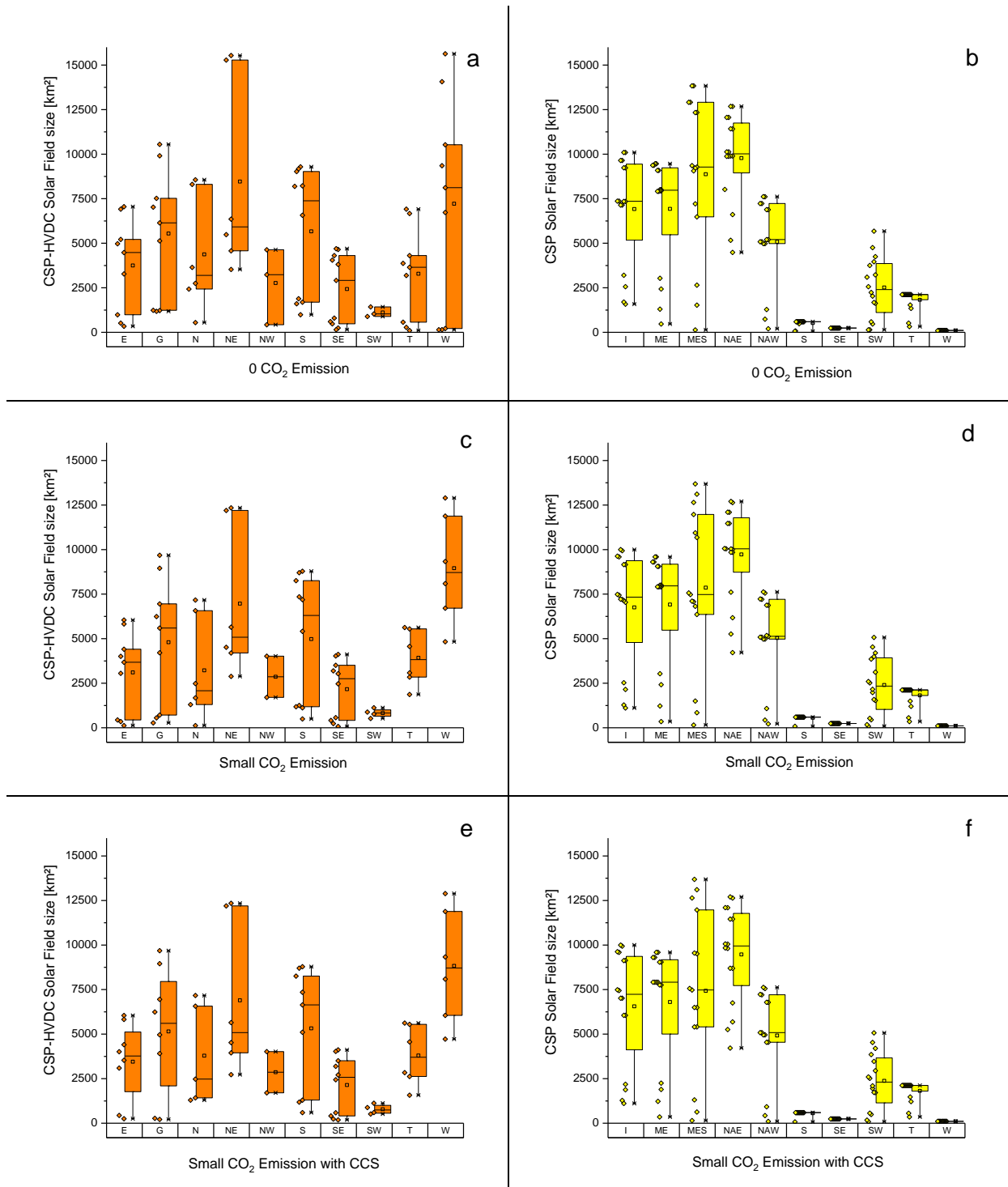
Figure 32: Solar field size – possible bandwidths of demand for land of CSP-HVDC and CSP